

RELATIVE SOIL IMPEDANCES BENEATH
ELECTRICAL PENETRATION WINGS FOR
THE MIDLAND AUXILIARY BUILDING

by

R. P. KENNEDY
R. H. KINCAID
D. A. WESLEY
R. D. THRASHER

prepared for:

CONSUMERS POWER COMPANY
JACKSON, MICHIGAN

March, 1982

8205180243

1. PURPOSE OF STUDY

The auxiliary building at the Midland Nuclear Generating Station is a reinforced concrete structure consisting of the main auxiliary building, the control tower, and the east and west electrical penetration wing areas. A schematic representation of this complex structure is presented in Figure 1-1. In order to assess the dynamic loadings on this structure due to earthquake ground motion, a lumped-mass, three-dimensional model (shown in Figure 1-2) has been developed for the auxiliary building complex (Reference 1). This model incorporates all important mass and stiffness characteristics of the structure and preserves the overall physical geometry of the building. Basically, the model consists of two main sticks representing the main auxiliary building and control tower with the remaining six sticks, in conjunction with a series of plate elements, modeling the east and west electrical penetration wing areas. The stiffness elements representing story stiffnesses account for the actual distributed shear, flexural, and axial stiffnesses of the seismic-resistant structural elements. Stiffness elements acting as rigid links model the horizontal diaphragms. These elements also link together horizontally and vertically all lumped masses in the model. The plate elements in the electrical penetration wing areas model the vertical south wall of this structure. Stiffness elements and lumped masses are used to model intermediate cross walls in the wing area.

Soil-structure interaction for this structure has been developed using elastic half-space, frequency-dependent impedance functions. The global soil impedances have been based on the full auxiliary building foundation geometry. Examination of Figure 1-3 show this building has a very complex foundation shape. Because this structure has a thick base mat with many large interior shear walls stiffening the foundation, it was judged that assuming the total structure base mat acts rigidly was an acceptable procedure for developing global soil compliances for the structure. However, because the electrical penetration wings are long

and narrow (Figures 1-1 to 1-3), there was concern that for North-South (N-S) excitation there might be some slight flexibility of the electrical penetration wing foundation relative to the main auxiliary/control tower foundation. Though this flexibility would not substantially affect the global soil impedances calculated by elastic half-space theory, flexing of the wings relative to the main auxiliary building and control tower might substantially influence in-structure floor response spectra calculated out in the wings. Therefore, in order to accurately define loadings and floor spectra in the wings, it may be necessary to correctly distribute the portion of overall soil spring stiffness that supports the wing area to the nodal points in the mathematical model representing the wing foundation rather than lump all the soil stiffness at a single location beneath the auxiliary building foundation.

Because of these concerns (Reference 2), a parametric study was conducted in order to determine the effect on spectra of the distribution of the soil impedance beneath the electrical penetration wings. Three cases were analyzed. The first case studied, defined as the global stiffness case, assumed that the soil compliance functions were developed using the overall structure foundation geometry and were located at the base mat centroid as shown in Figure 1-3. No soil springs were located beneath the wing areas for this case. In the second case, defined as the lower bound relative wing stiffness case, a procedure was developed that calculated the lowest reasonable relative stiffnesses for the springs beneath the wing areas. Soil springs were then distributed beneath the wing areas and under the main auxiliary building/control tower foundation as shown schematically in Figure 1-4. Equilibrium of the overall model was considered in order to ensure this case had the same global soil characteristics as defined by case one above. The final case, defined as the upper bound relative wing stiffness case, used a procedure that calculated the highest reasonable relative stiffness for soil springs under the wings. As in case two, the soil stiffnesses beneath the auxiliary building/control tower foundation were adjusted to maintain the same global model characteristics defined by case one above. Using these models, comparisons of in-structure floor response spectra, peak

acceleration, and peak displacements for each of the three models were made in order to determine the importance of modeling the soil beneath the wings.

Section 2 of this report presents the methodology used to develop the soil stiffnesses for each of these three cases. Comparisons of in-structure floor response spectra, peak displacements, and accelerations at typical locations in the building for each of the three cases studied, are presented in Section 3. Section 4 summarizes all important results and presents conclusions regarding sensitivity of the seismic response and the necessity of correctly modeling the soil beneath the wings.

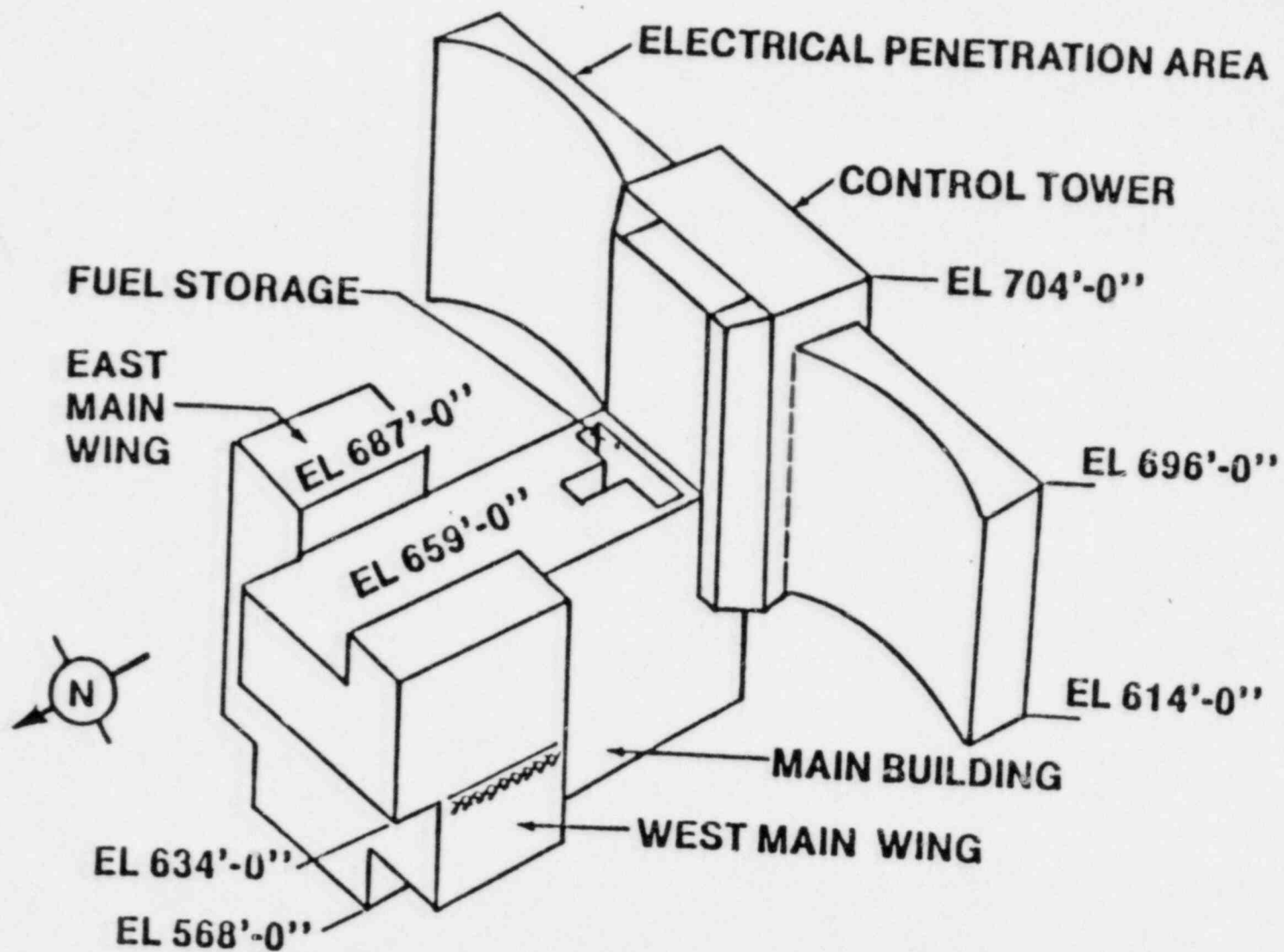


FIGURE 1-1: SCHEMATIC REPRESENTATION OF THE MIDLAND AUXILIARY BUILDING COMPLEX

AUXILIARY BUILDING SEISMIC MODEL

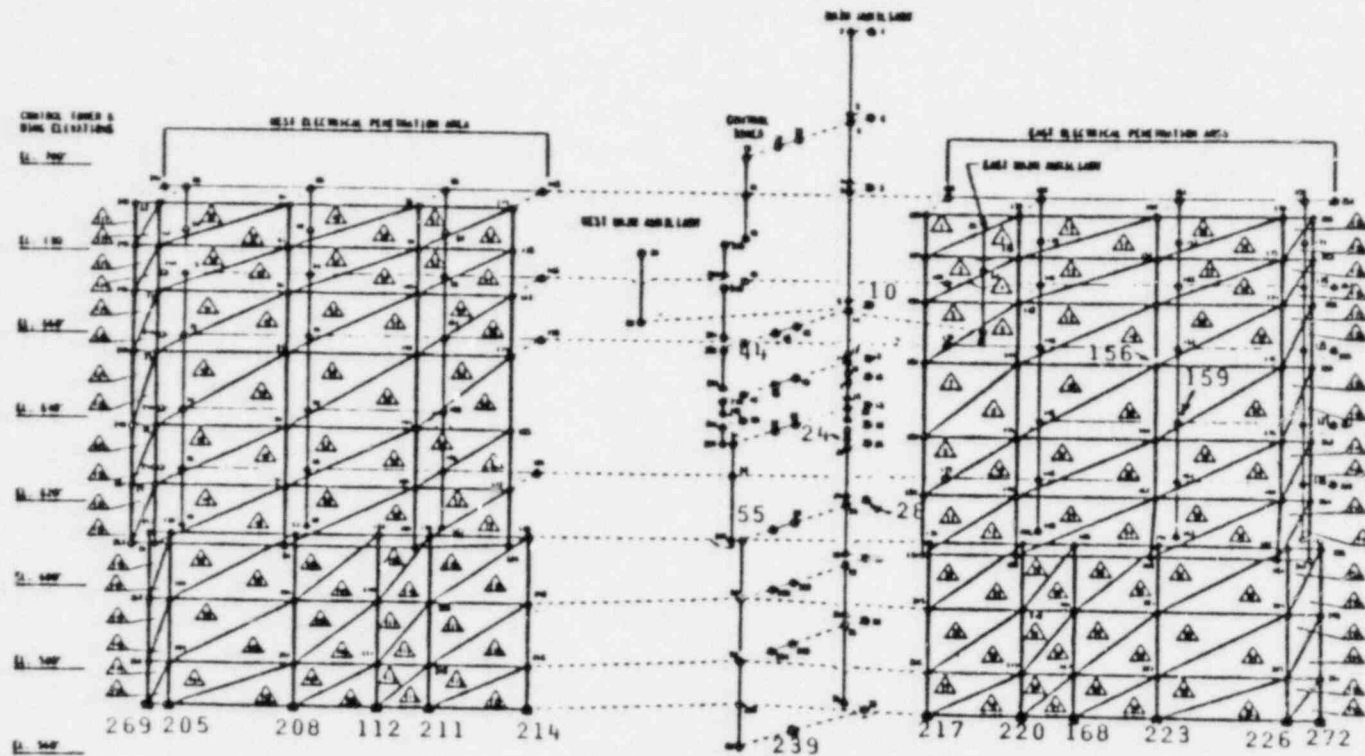


FIGURE 1-2: MATHEMATICAL MODEL OF AUXILIARY BUILDING

BECHTEL

WIND AND PLANT UNITS 1 & 2
CONSUMERS POWER COMPANY

AUXILIARY BUILDING
3-D SEISMIC MODEL
PLATE LAYOUT

1.000

AUXILIARY BUILDING SCHEMATIC PLAN

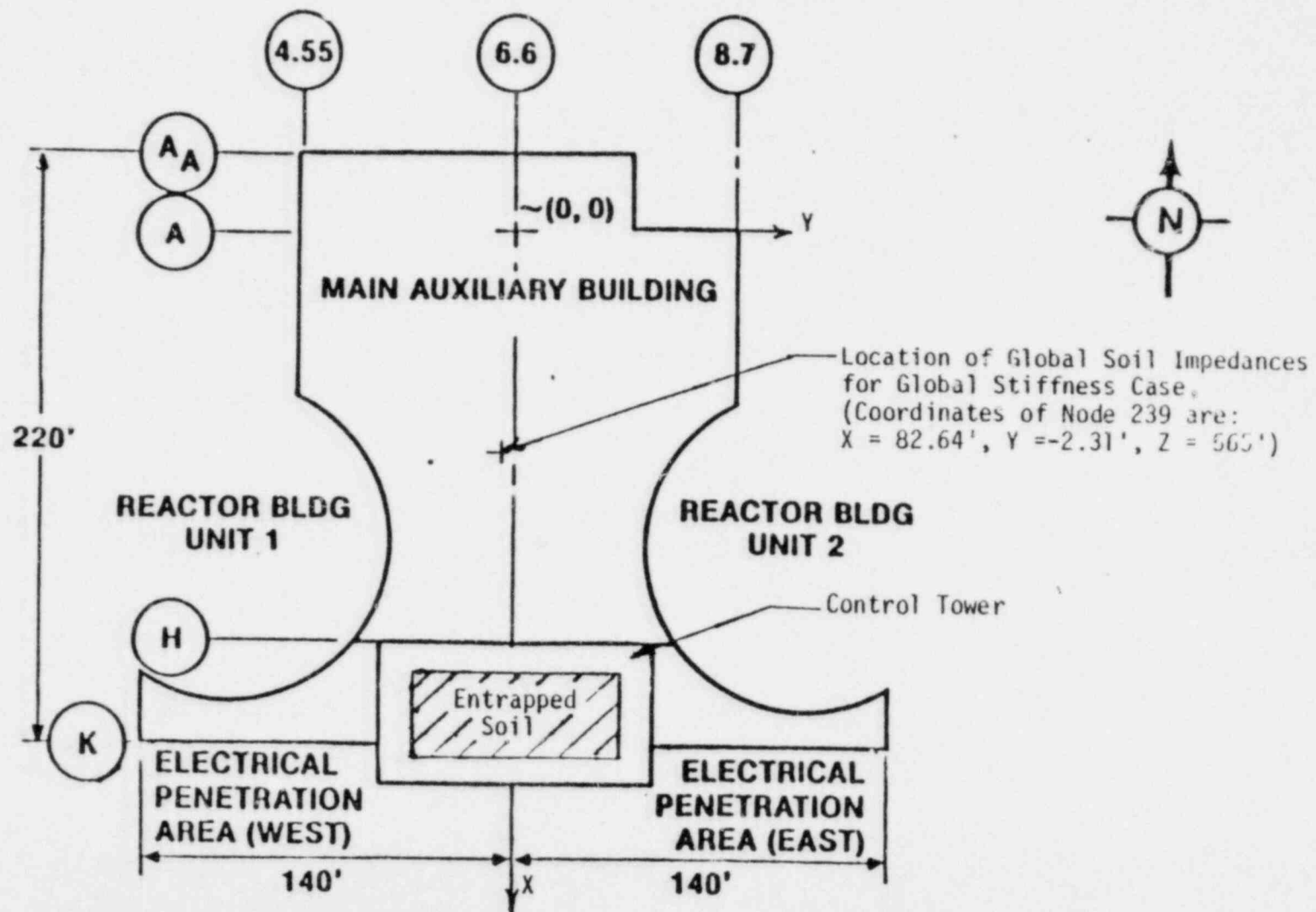


FIGURE 1-3: SCHEMATIC REPRESENTATION OF AUXILIARY BUILDING FOUNDATION

AUXILIARY BUILDING

(With Conceptual Seismic Model)

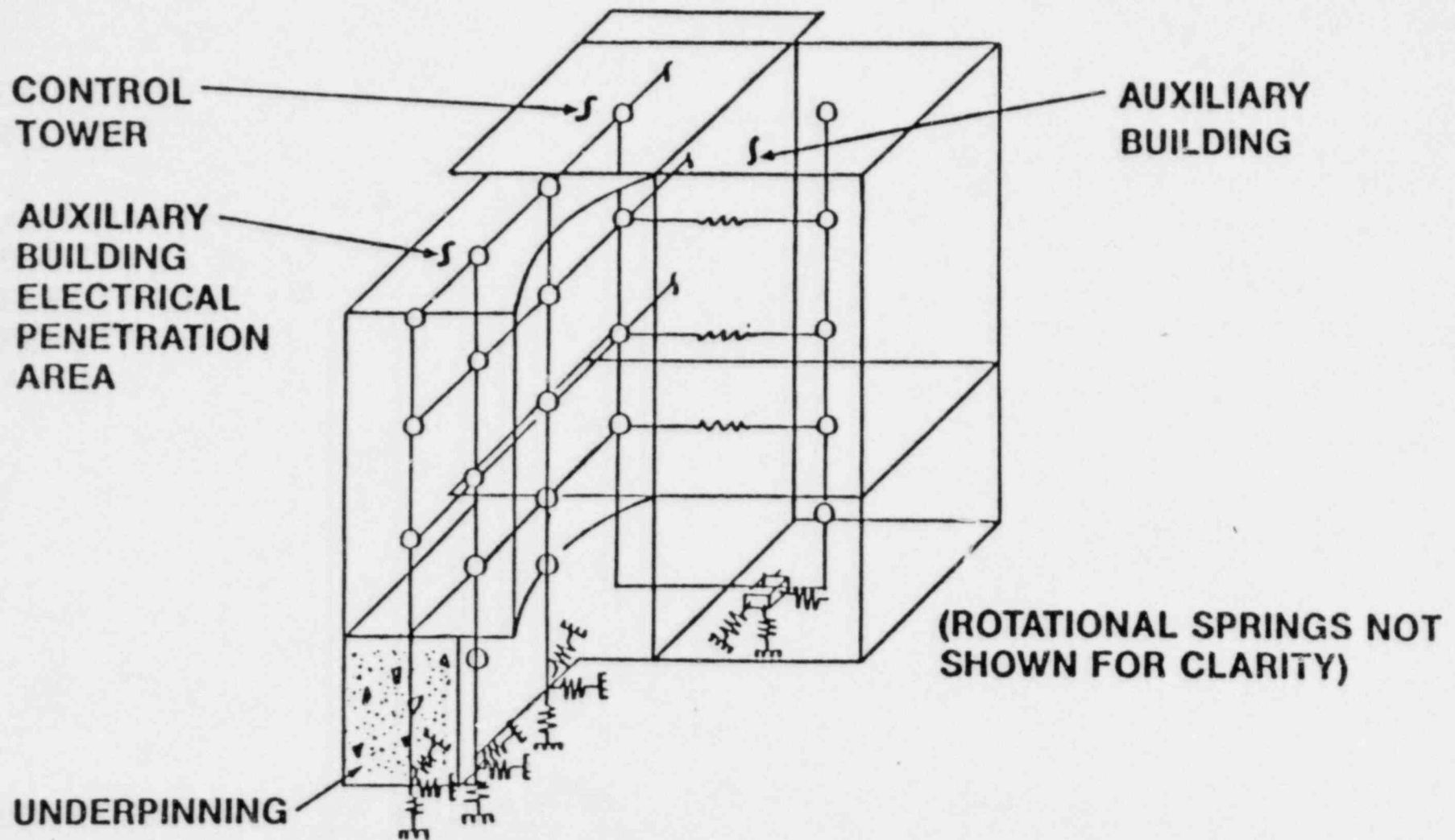


FIGURE 1-4: SCHEMATIC REPRESENTATION OF AUXILIARY BUILDING MATHEMATICAL MODEL SHOWING PLACEMENT OF SOIL SPRINGS BENEATH THE PENETRATION WINGS

2. ANALYTICAL APPROACH

2.1 DEVELOPMENT OF GLOBAL SOIL IMPEDANCE

Soil impedances under the auxiliary building were developed based on frequency-dependent, elastic half-space equations, as shown in Table 2-1, with soil springs modeling the real part of the soil compliances and viscous dashpots modeling the imaginary part. These equations are based on relationships presented in Reference 3. The use of an elastic half-space formulation required the development of an effective soil shear modulus for the half-space, G_{eff} , to use in determining the soil impedances. Because the soil profile beneath the auxiliary building is comprised of differing soil layers of varying stiffness and shear wave velocities, a layered site analysis using the Program CLASSI (Reference 4) was conducted to determine best estimate soil effective elastic half-space shear moduli. Since this procedure will be discussed in detail in a later SMA report on the Seismic Margin Evaluation for the Midland Plant, it will not be presented herein. CLASSI layered site analyses demonstrated that effective shear moduli of 7,100 ksf for the two horizontal translation and torsional dof and 8,600 ksf for the rocking and vertical dof adequately represented the site characteristics for the best estimate soil case.

The projected foundation geometry for the auxiliary building at elevation 562 feet is shown in Figure 1-3. Within the area shown as the control tower foundation, there is a large mass of entrapped soil. In developing the effective rectangular foundation properties for the auxiliary building complex, this soil was considered to act as part of the foundation for horizontal translation and torsional dof. For rocking and vertical translation, the foundation geometry was considered to consist of the base mat and spread footings only with no consideration given to the entrapped soil. The centroidal location for placement of the soil springs and dashpots were calculated based on the actual foundation geometry for all degrees-of-freedom (dof). This location is

shown in Figure 1-3 for the global stiffness case and corresponds to node point 239 in the mathematical model shown in Figure 1-2.

The frequency-dependent, elastic half-space equations presented in Table 2-1 were used to define global soil impedances. The frequency-dependent coefficients in these formulations were developed based on References 5, 6 and 7. A Poisson's ratio of $\gamma = 0.42$ and unit weight of $\alpha = 135$ pcf for the soil was used in all cases. Using this data in conjunction with the effective soil moduli and equivalent rectangles based on actual foundation geometry discussed above, non-embedded soil springs and dashpots were developed for the structure. These soil impedances are presented in Table 2-2. When determining the dashpots values shown in Table 2-2, soil radiation damping was limited to 75% of theoretical elastic half space damping for horizontal translation and torsional dof and to 50% of theoretical elastic half space damping for rocking dof. These conservative limitations on soil geometric damping were based on comparisons of soil radiation damping determined from the CLASSI layered site analysis to soil radiation damping based on elastic half-space theory.

The auxiliary building is embedded in the surrounding soil approximately 60 feet on all sides. The stiffening effects of the side soil were considered using a frequency-dependent embedment approach presented in Reference 1. Table 2-2 presents the calculated embedment factors as a multiplier to be applied to the non-embedded, elastic half-space spring stiffnesses and dashpots. Table 2-2 also presents the final global embedded spring stiffnesses and dashpots for the auxiliary building complex. Note in this table that the embedded dashpots have been adjusted to account for 5 percent soil hysteretic damping. The global soil springs and dashpot values are applied at the centroidal location shown in Figure 1-3 in the auxiliary building mathematical model. The spring and dashpot values presented in Table 2-2 are the basis for the global stiffness case.

2.2 LOWER BOUND RELATIVE WING STIFFNESS CASE

Figure 2-1 presents a plan view of the auxiliary building foundation geometry used to develop the lower bound relative wing stiffness case. This procedure assumes that for the translation dof beneath the wing area, the proportion of the overall global stiffness to be applied beneath the wing is given by:

$$K_W (X,Y,Z) = \frac{A_W}{A_T} K_G (X,Y,Z) \quad (2-1)$$

where:

$K_G(X,Y,Z)$ = The global translational (X,Y, or Z direction) soil spring stiffness as determined in Section 2.1 above.

A_T = Total foundation plan area including the wings.

A_W = Foundation plan area of a single wing.

This procedure assumes the maximum possible interaction between the wing foundation and the main auxiliary building/control tower foundation. This assumption overemphasizes the interaction effect on the wing stiffnesses since the soil beneath the outer extremities of the wings should not be influenced much by soil stresses beneath the main auxiliary building. The wings actually would be more independent of the main auxiliary building foundation than this procedure assumes with a larger portion of the overall soil stiffness occurring beneath them. Consequently, this procedure results in a lower-bound estimate of the relative wing stiffnesses.

For rocking of the structure in the North-South (N-S) direction (about the Y axis), the rocking stiffness beneath the wing area, $K_{\psi_W}(N-S)$, is determined in the following manner. First, the embedded elastic half space rocking stiffness, $K_{\psi_W}^*(N-S)$, and vertical stiffness, $K_W^*(Z)$, are calculated for the wing area alone. These stiffnesses are developed assuming that the wing area, A_W , (see Figure 2-1) acts independently from the rest of the auxiliary building foundation. The rocking stiffness $K_{\psi_W}^*(N-S)$ and vertical stiffness $K_W^*(Z)$ of the wing are determined based on the area and shape of the wing using the elastic half space stiffnesses presented in Table 2-1, G_{eff} as previously defined in Section 2.1, and the embedment factors from Table 2-2. The rocking stiffness $K_{\psi_W}(N-S)$ is then factored down proportional to the ratio $\frac{K_W(Z)}{K_W^*(Z)}$ in order to determine the actual rocking stiffness $K_{\psi_W}(N-S)$ beneath the wing area for the lower bound relative wing stiffness case. Note that the term $K_W(Z)$ is defined by Equation 2-1 above and represents the lower bound relative wing stiffness in the vertical direction. This factoring process assumes that the rotational soil stiffness, beneath the wing area is proportional to the vertical soil stiffness determined by tributary area considerations and again overemphasizes interaction effects between the main auxiliary building and the wing areas. This relationship for the wing rocking spring stiffness, $K_{\psi_W}(N-S)$ may be expressed as follows:

$$K_{\psi_W}(N-S) = \frac{K_W(Z)}{K_W^*(Z)} K_{\psi_W}^*(N-S) \quad (2-2)$$

Details of these calculations for translational and rocking stiffnesses are presented in Appendix A. Rocking stiffnesses in the East-West (E-W) and local torsional stiffnesses under the wings were not developed since the wing foundation is extremely stiff for these dof and local response of the wings is not expected to be significantly influenced by modeling soil springs beneath the wings for these directions.

Once lower bound relative wing stiffnesses were determined for each of the wing areas shown in Figure 2-1, nodal springs were developed for application beneath the wings in the three-dimensional mathematical model of the auxiliary building shown in Figure 1-2. These nodal springs were determined from the overall wing translational and rocking stiffnesses defined by Equations 2-1 and 2-2 above, based on the contributory area of each nodal point beneath the wings. The nodal translational springs developed for the electrical penetration wings are applied at node points 217, 220, 168, 223, 226, and 272 for the east wing and at nodes 269, 205, 208, 112, 211, and 214 beneath the west wing. The remaining soil stiffness is applied at node 239. However, in order to maintain the same global model characteristics defined by the global stiffness case discussed in Section 2.1, it was necessary to recalculate the magnitude and centroidal location of the soil springs, dashpots, and base mat masses defined beneath the auxiliary building/control tower portion of the model. In order to maintain the same center of rotation as defined by the global stiffness case, equilibrium considerations show that the centroidal location of node 239 must shift to the new coordinates shown in Figure 2-1. Comparison of Figure 2-1 to Figure 1-3 shows that node 239 has shifted approximately 9.9 feet to the north of the location defined in the global stiffness case. Details of these calculations are given in Appendix A. Table 2-3 presents the lower bound relative wing stiffnesses used with the auxiliary building model.

2.3 Upper Bound Relative Wing Stiffness Case

The intent of this bounding procedure was to define the maximum possible relative soil spring stiffness beneath the wing areas. Maximum relative soil spring stiffnesses beneath the wing area are calculated whenever the minimum possible interaction effects between the main auxiliary/control tower and the wing areas occur. A simple procedure based on elastic half space theory was used to develop upper bound relative soil spring stiffness for this case.

Figure 2-2 presents a plan view of the auxiliary building foundation geometry used to develop the upper bound relative wing stiffness case. A composite foundation for the electrical penetration

wings and control tower was considered to be defined by the area enclosed by the dashed line in this figure. This idealized foundation includes the area of the east and west electrical penetration wing foundations and a foundation strip running the length of the control tower foundation equal in width to the electrical penetration wing foundations. This composite foundation represents a realistic bound on the minimum portion of the overall auxiliary building/control tower foundation which would be expected to interact with the wing areas. This composite foundation was used to develop relative soil stiffnesses beneath the wing areas. In reality there would be more interaction between the rest of the auxiliary building foundation and the wing areas than this composite footing assumes and the relative soil stiffnesses beneath this composite footing would be smaller in magnitude than those determined using this procedure. Relative stiffnesses beneath the wing areas were then calculated based on the preceding formulation for the upper bound relative wing stiffness case. This may be expressed as:

$$K_w(X,Y,Z, \psi(N-S)) = \frac{A_w}{A_c} K_c(X,Y,Z, \psi(N-S)) \quad (2-3)$$

where:

$K_w(X,Y,Z, (N-S)) =$ The translational (X,Y,X) or rotational ($\psi(N-S)$) relative soil spring stiffness based on the area of one wing.

$K_c(X,Y,Z, (N-S)) =$ The translational (X,Y,Z) or rotational ($\psi(N-S)$) soil spring stiffness based on the geometry of the composite wing area, A_c , effective soil shear modulus, G_{eff} , and embedded elastic half space theory.

A_c = Foundation plan area of composite wing as shown in Figure 2-2.

A_w = Foundation plan area of a single wing.

Once upper bound relative wing stiffnesses were determined for each of the wing areas shown in Figure 2-2, nodal springs were again developed for application beneath the wings in the three-dimensional mathematical model of the auxiliary building shown in Figure 1-2. These nodal springs were determined from the overall wing translational and rocking stiffnesses defined by Equation 2-3 above using the procedure discussed in Section 2.2.

Table 2-3 presents a tabulation of the nodal stiffnesses developed for this case. The stiffnesses beneath the wing areas are approximately a factor of 3 and 5 higher (translational and rocking dof, respectively) than those presented for the lower bound relative wing stiffness case. The stiffness and location of the soil springs beneath the main auxiliary building/control tower was again adjusted for this case in order to maintain the same overall soil stiffness as defined by the global stiffness case. Figure 2-2 shows the location of node 239 for this case. Because of the relatively large, vertical wing stiffnesses, this nodal location has now shifted about 38.7 feet north of the original location as defined by the global stiffness case (Figure 1-3) in order to maintain the correct center of rotation. Details for these calculations may be found in Appendix A.

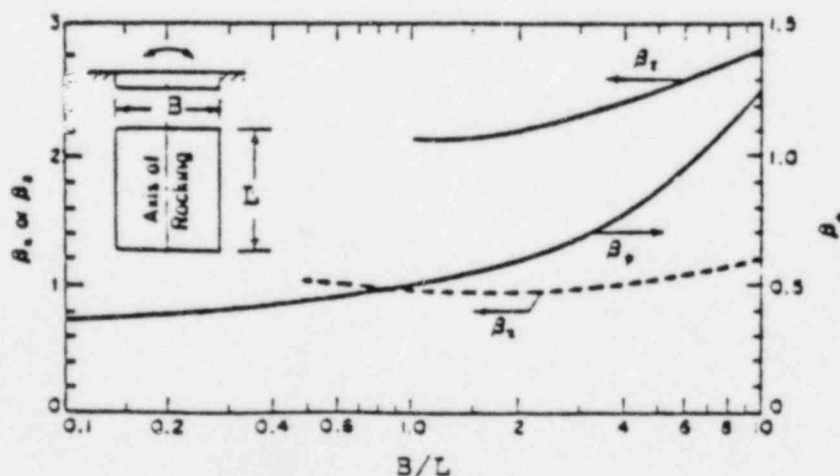
TABLE 2-1
FREQUENCY DEPENDENT ELASTIC HALF SPACE IMPEDANCE

<u>Motion</u>	<u>Equivalent Spring Constant</u>	<u>Equivalent Damping Coefficient</u>
Horizontal	$k_x = k_1 2(1+\nu)GB_x\sqrt{BL}$	$c_x = c_1 k_x(\text{static})R\sqrt{\rho/G}$
Rocking	$k_\psi = k_2 \frac{G}{1-\nu} B_\psi B^2 L$	$c_4 = c_2 k_\psi(\text{static})R\sqrt{\rho/G}$
Vertical	$k_z = k_3 \frac{G}{1-\nu} B_z\sqrt{BL}$	$c_z = c_3 k_z(\text{static})R\sqrt{\rho/G}$
Torsion	$k_t = k_4 16GR^3/3$	$c_t = c_4 k_t(\text{static})R\sqrt{\rho/G}$

in which:

- ν = Poisson's ratio of foundation medium,
- G = shear modulus of foundation medium,
- R = radius of the circular base mat,
- ρ = density of foundation medium,
- B = width of the base mat in the plane of horizontal excitation;
- L = length of the base mat perpendicular to the plane of horizontal excitation;

$k_1, k_2, k_3, k_4,$
 c_1, c_2, c_3, c_4 = frequency dependent coefficients modifying the static stiffness or damping



Constants β_x , β_y and β_z for
Rectangular Bases

TABLE 2-2

GLOBAL SOIL STIFFNESS AND DAMPING
CONSTANTS FOR THE AUXILIARY BUILDING COMPLEX

A) SPRING CONSTANTS

Motion	Non Embedded Soil Stiffness	Embedment Factor	Embedded Soil Stiffness
Translational			
North-South	$3.21 \cdot 10^6 \text{ k/ft}$	1.11	$3.56 \cdot 10^6 \text{ k/ft}$
East-West	$3.36 \cdot 10^6 \text{ k/ft}$	1.10	$3.70 \cdot 10^6 \text{ k/ft}$
Vertical	$3.64 \cdot 10^6 \text{ k/ft}$	1.09	$3.97 \cdot 10^6 \text{ k/ft}$
Rotational			
North-South	$3.73 \cdot 10^{10} \text{ k-ft/rad}$	1.24	$4.63 \cdot 10^{10} \text{ k-ft/rad}$
East-West	$2.85 \cdot 10^{10} \text{ k-ft/rad}$	1.22	$3.48 \cdot 10^{10} \text{ k-ft/rad}$
Torsional	$3.48 \cdot 10^{10} \text{ k-ft/rad}$	1.21	$4.21 \cdot 10^{10} \text{ k-ft/rad}$

B) RADIATION DAMPING COEFFICIENTS

Motion	Non Embedded Damping Coefficient	Embedment Factor	Embedded Damping Coefficient*
Translational			
North-South	$1.12 \cdot 10^5 \text{ k-sec/ft}$	1.25	$1.60 \cdot 10^5 \text{ k-sec/ft}$
East-West	$1.19 \cdot 10^5 \text{ k-sec/ft}$	1.24	$1.69 \cdot 10^5 \text{ k-sec/ft}$
Vertical	$2.54 \cdot 10^5 \text{ k-sec/ft}$	1.11	$2.97 \cdot 10^5 \text{ k-sec/ft}$
Rotational			
North-South	$4.53 \cdot 10^8 \text{ k-ft-sec}$	1.44	$9.07 \cdot 10^8 \text{ k-ft-sec}$
East-West	$2.03 \cdot 10^8 \text{ k-ft-sec}$	1.46	$5.01 \cdot 10^8 \text{ k-ft-sec}$
Torsional	$3.79 \cdot 10^8 \text{ k-ft-sec}$	1.49	$8.03 \cdot 10^8 \text{ k-ft-sec}$

*Includes 5% Soil Hysteretic Damping

TABLE 2-3
NODAL SPRING STIFFNESS FOR
LOWER AND UPPER BOUND RELATIVE WING STIFFNESS CASES

Node Number	Direction	Motion	Lower Bound Relative Wing Stiffness Case	Upper Bound Relative Wing Stiffness Case
214,217	N-S E-W Vertical N-S	Translation Translation Translation Rocking	$4.17 \cdot 10^4$ $4.33 \cdot 10^4$ $5.00 \cdot 10^7$ $1.02 \cdot 10^7$	$1.41 \cdot 10^5$ $1.25 \cdot 10^5$ $1.53 \cdot 10^7$ $5.06 \cdot 10^7$
211,220	N-S E-W Vertical N-S	Translation Translation Translation Rocking	$4.49 \cdot 10^4$ $4.67 \cdot 10^4$ $5.39 \cdot 10^7$ $1.10 \cdot 10^7$	$1.52 \cdot 10^5$ $1.35 \cdot 10^5$ $1.65 \cdot 10^7$ $5.46 \cdot 10^7$
112,168	N-S E-W Vertical N-S	Translation Translation Translation Rocking	$1.18 \cdot 10^4$ $1.23 \cdot 10^4$ $1.42 \cdot 10^6$ $2.90 \cdot 10^6$	$4.00 \cdot 10^4$ $3.56 \cdot 10^4$ $4.35 \cdot 10^7$ $1.44 \cdot 10^7$
208,223	N-S E-W Vertical N-S	Translation Translation Translation Rocking	$2.50 \cdot 10^4$ $2.60 \cdot 10^4$ $3.01 \cdot 10^6$ $6.13 \cdot 10^6$	$8.47 \cdot 10^4$ $7.53 \cdot 10^4$ $9.20 \cdot 10^7$ $3.04 \cdot 10^7$
205,226	N-S E-W Vertical N-S	Translation Translation Translation Rocking	$2.18 \cdot 10^4$ $2.27 \cdot 10^4$ $2.62 \cdot 10^6$ $5.35 \cdot 10^6$	$7.38 \cdot 10^4$ $6.57 \cdot 10^4$ $8.02 \cdot 10^7$ $2.65 \cdot 10^7$
269,272	N-S E-W Vertical N-S	Translation Translation Translation Rocking	$5.40 \cdot 10^3$ $5.61 \cdot 10^3$ $6.48 \cdot 10^6$ $1.32 \cdot 10^6$	$1.82 \cdot 10^4$ $1.62 \cdot 10^4$ $1.98 \cdot 10^6$ $6.56 \cdot 10^6$
239	N-S E-W Vertical N-S E-W Torsion	Translation Translation Translation Rocking Rocking Rocking	$3.26 \cdot 10^6$ $3.38 \cdot 10^6$ $3.61 \cdot 10^{10}$ $3.20 \cdot 10^{10}$ $4.23 \cdot 10^{10}$ $3.68 \cdot 10^{10}$	$2.54 \cdot 10^6$ $2.79 \cdot 10^6$ $2.86 \cdot 10^{10}$ $2.62 \cdot 10^{10}$ $3.05 \cdot 10^{10}$ $2.39 \cdot 10^{10}$

NOTE: 1. Units on translational springs are kip/ft
2. Units on rotational springs are kip-ft/rad

AUXILIARY BUILDING SCHEMATIC PLAN

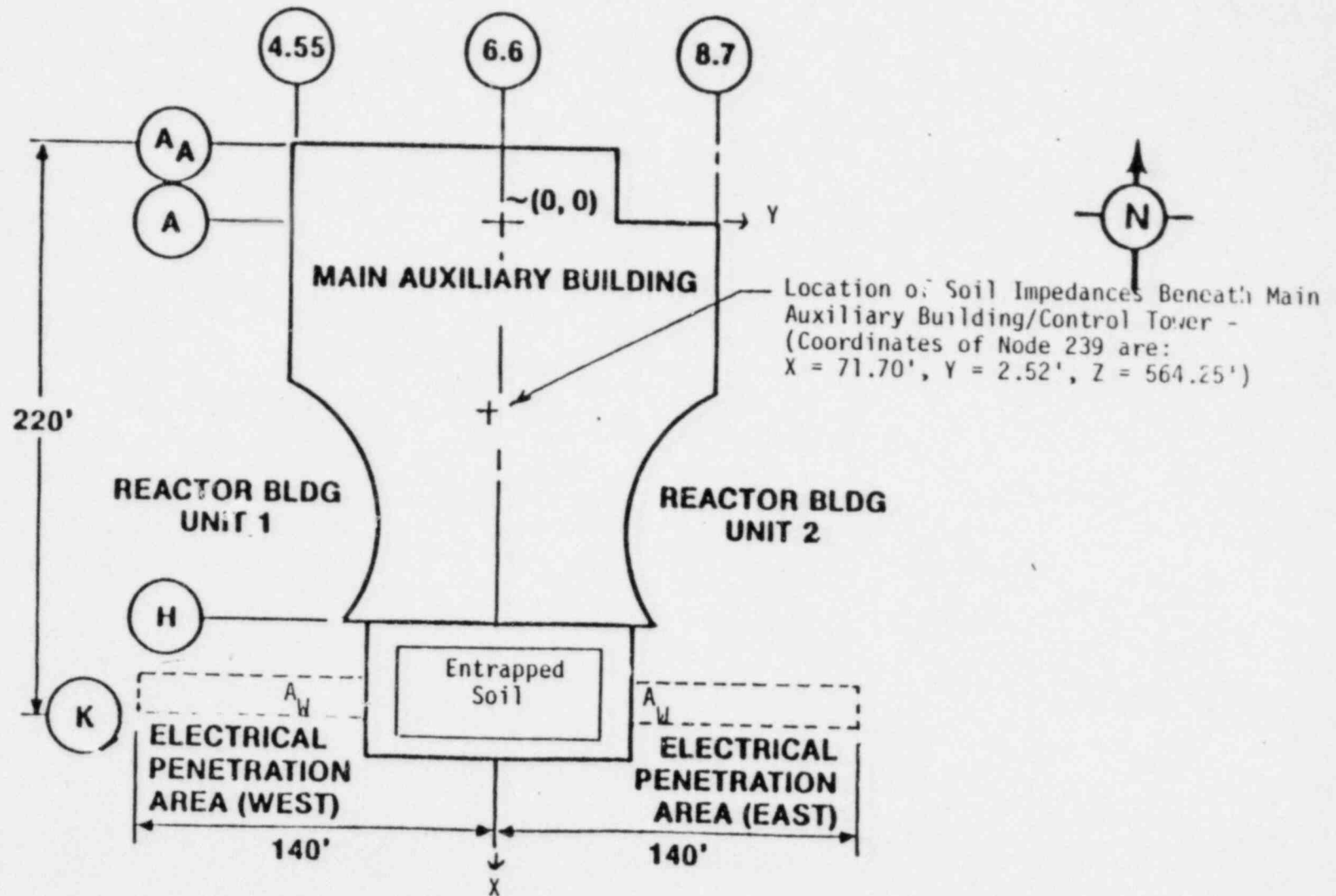


FIGURE 2-1. SCHEMATIC REPRESENTATION OF AUXILIARY BUILDING FOUNDATION USED TO DEVELOP LOWER BOUND RELATIVE WING STIFFNESS CASE

AUXILIARY BUILDING SCHEMATIC PLAN

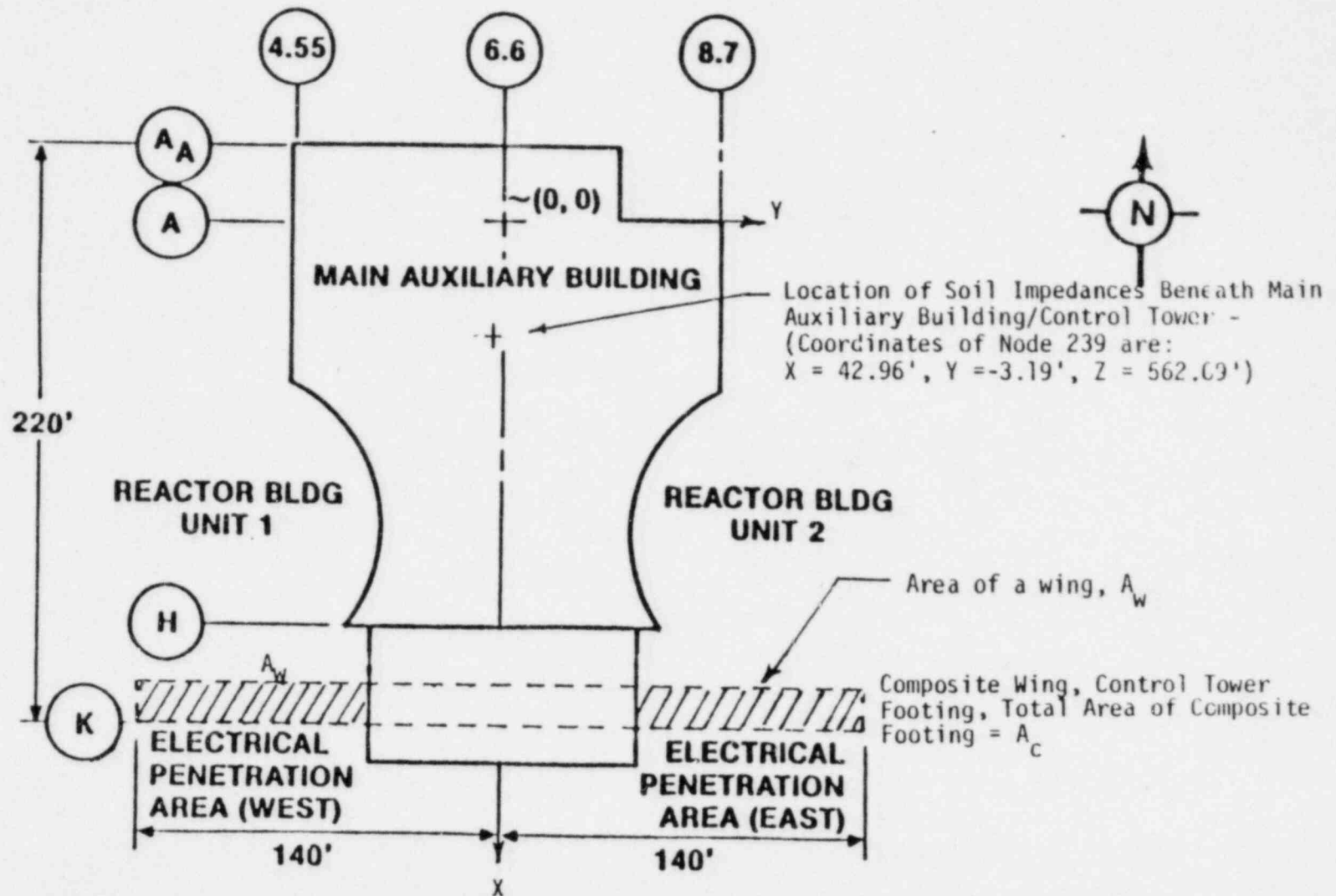


FIGURE 2-2. SCHEMATIC REPRESENTATION OF AUXILIARY BUILDING FOUNDATION USED TO DEVELOP UPPER BOUND RELATIVE WING STIFFNESS CASE

3. SEISMIC RESPONSE RESULTS

3.1 APPROACH

In-structure (or floor) response spectra were developed for each of the three soil cases studied. In-structure response spectra were selected as the primary basis for comparison of the effects due to wing soil stiffness modelling assumptions since differences in the response spectra are more pronounced than in-structure accelerations or loads. However, peak accelerations and relative displacements were also checked at selected locations. Because of the flexibility of the electrical penetration wings under N-S excitation, this direction of excitation and corresponding structural response represented the greatest potential for significant differences in floor response spectra between the different cases. In order to develop the floor response spectra, modal characteristics of the structure were required. Table 3-1 presents the fundamental frequencies for the X, Y, and Z directions for each of the three soil cases. Only minor shifts in frequency are evident. This demonstrates that placement of soil stiffness beneath wings does not significantly affect the global characteristics of the model and implies that the base mat of the structure is essentially translating and rotating as a rigid body in all cases.

In-structure response spectra were developed using modal superposition time history analysis on Computer Program MODSAP (Reference 8). Composite modal damping values associated with each mode were developed based on the Tsai Method (Reference 9) using Program SOILST (Reference 10). A subsequent report by SMA will describe the development of the composite modal damping values and therefore the damping values used and their basis will not be presented here.

An artificial earthquake time history scaled to a peak acceleration of approximately 0.13g which essentially enveloped the ground response spectra for the original ground surface (Reference 11) was used

in all cases to excite the structure. A comparison of the time history response spectra with the design ground response spectra is shown in Figure 3-1 for 5% and 20% of critical damping.

Typical locations in the structure were chosen for development of floor response spectra, peak relative displacements, and peak absolute accelerations. The locations studied were (see Figure 1-2):

1. Control Tower - Elevation 614 ft - Node 55
2. Control Tower - Elevation 659 ft - Node 44
3. Main Auxiliary Building - Elevation 614 ft - Node 28
4. Main Auxiliary Building - Elevation 628.5 ft - Node 24
5. Main Auxiliary Building - Elevation 659 ft - Node 10
6. East Penetration Wing - Elevation 642.6 ft - Node 159
7. East Penetration Wing - Elevation 674.5 ft - Node 156

3.2 COMPARISON OF IN-STRUCTURE RESPONSE SPECTRA

Figures 3-2 to 3-8 show a comparison of 2 percent critical damping in-structure floor response spectra developed for the locations presented in the previous section for each of the three cases studied. These spectra were developed for N-S structural response under N-S ground motion. The spectra are nearly identical in each case. However, the following trends may be noted from these spectra. First, in the region of the fundamental N-S frequency of 2.7 hertz, the lower bound relative wing stiffness case and global stiffness case predict slightly higher spectral accelerations than the upper bound relative wing stiffness case. In the higher frequency regions of the spectra (4 to 10 hertz) range, results show that for all three cases approximately the same spectral response is obtained throughout this frequency region with the exception of node 156 (Figure 3-8). For node 156, the lower bound relative wing stiffness case and global stiffness case predict higher responses than the upper bound relative wing stiffness case. The spectra at a given elevation all return to approximately the same ZPA for each of the three cases studied.

Table 3-2 presents a comparison of peak relative displacements and peak absolute accelerations for these same locations for the soil cases studied. Results are almost identical for all cases studied at a specific elevation. The lower bound relative wing stiffness and global stiffness cases agree within 5% of each other at all locations and tend to have slightly higher responses than does the upper bound relative stiffness case (on the average about 5% higher for acceleration and 2% higher for displacement).

Maximum differences in structural response would be expected to occur under N-S excitation because this direction represents the greatest potential flexibility of electrical penetration wings. Other directions would be expected to show lesser differences. Because of the excellent comparisons shown for in-structure response spectra, peak relative displacements, and peak absolute accelerations for the three cases studied under N-S excitation, it was determined that additional work considering response in other directions was not required.

TABLE 3-1
FUNDAMENTAL STRUCTURE FREQUENCIES FOR CASES STUDIED

Mode	Direction	Global Stiffness Case	Lower Bound Relative Wing Stiffness Case	Upper Bound Relative Wing Stiffness Case
1	East-West	2.60	2.63	2.59
2	North-South	2.69	2.70	2.67
5	Vertical	3.67	3.71	3.72

TABLE 3-2

COMPARISON OF PEAK RELATIVE DISPLACEMENTS AND PEAK ABSOLUTE ACCELERATION
FOR CASES STUDIED

LOCATION			Peak Relative Displacements (inches)			Peak Absolute Accelerations (G'S)		
			Global Stiffness Case	Lower Bound Relative Wing Stiffness Case	Upper Bound Relative Wing Stiffness Case	Global Stiffness Case	Lower Bound Relative Wing Stiffness Case	Upper Bound Relative Wing Stiffness Case
Node	Eleva- tion	Building						
55	614'	Control Tower	0.160	0.159	0.159	0.142	0.145	0.139
44	659	Control Tower	0.219	0.220	0.218	0.165	0.167	0.156
28	614	Main Aux.	0.165	0.165	0.165	0.145	0.148	0.143
24	628.5	Main Aux.	0.181	0.180	0.180	0.150	0.151	0.145
10	659	Main Aux.	0.212	0.213	0.211	0.163	0.162	0.160
159	642.6	East Wing	0.249	0.234	0.230	0.181	0.175	0.166
156	674.5	East Wing	0.300	0.298	0.294	0.246	0.259	0.243

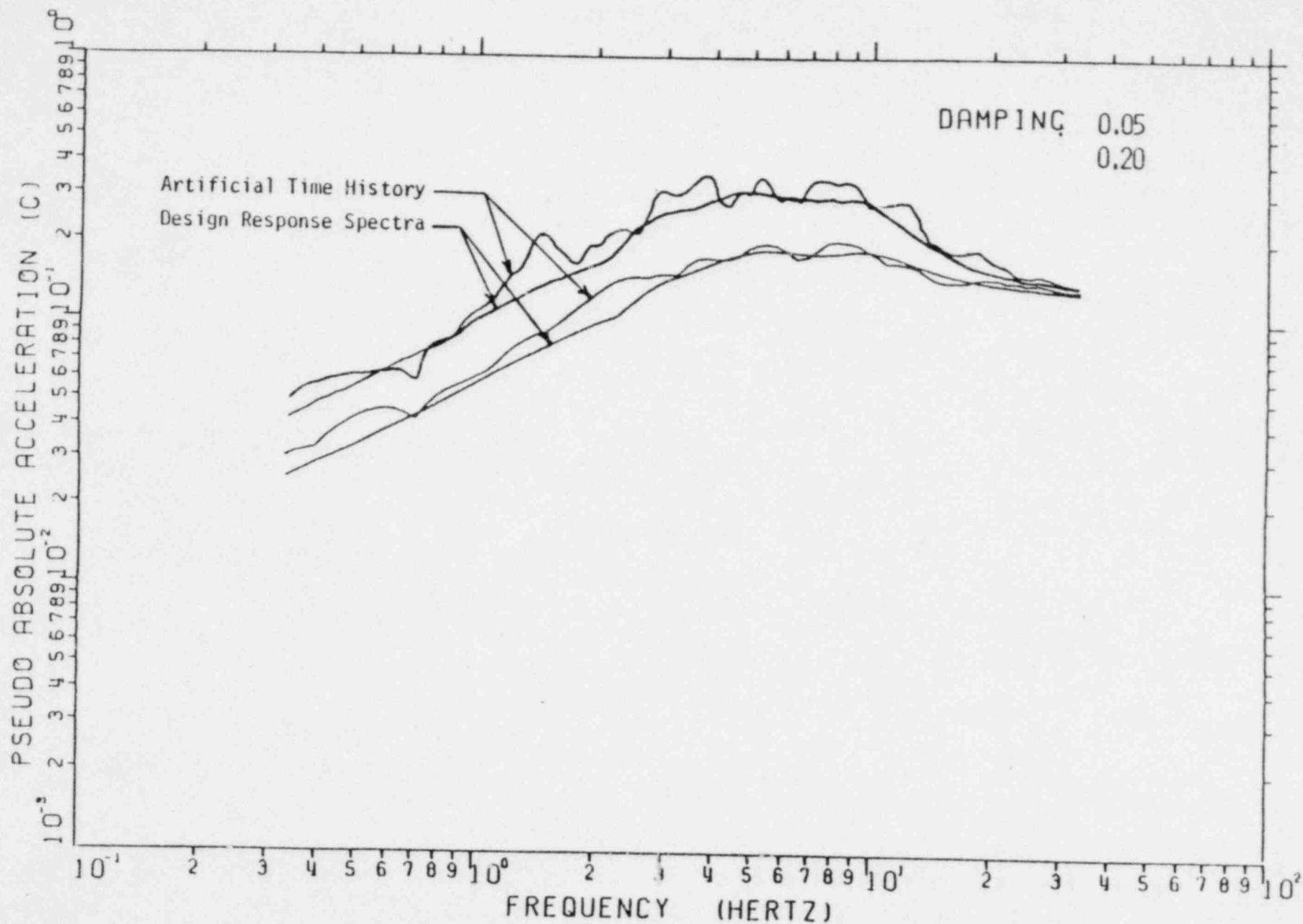


FIGURE 3-1: COMPARISON OF 5 AND 20 PERCENT CRITICAL DAMPING RESPONSE SPECTRA
GENERATED FROM ARTIFICIAL TIME HISTORY AND DESIGN TARGET RESPONSE SPECTRA

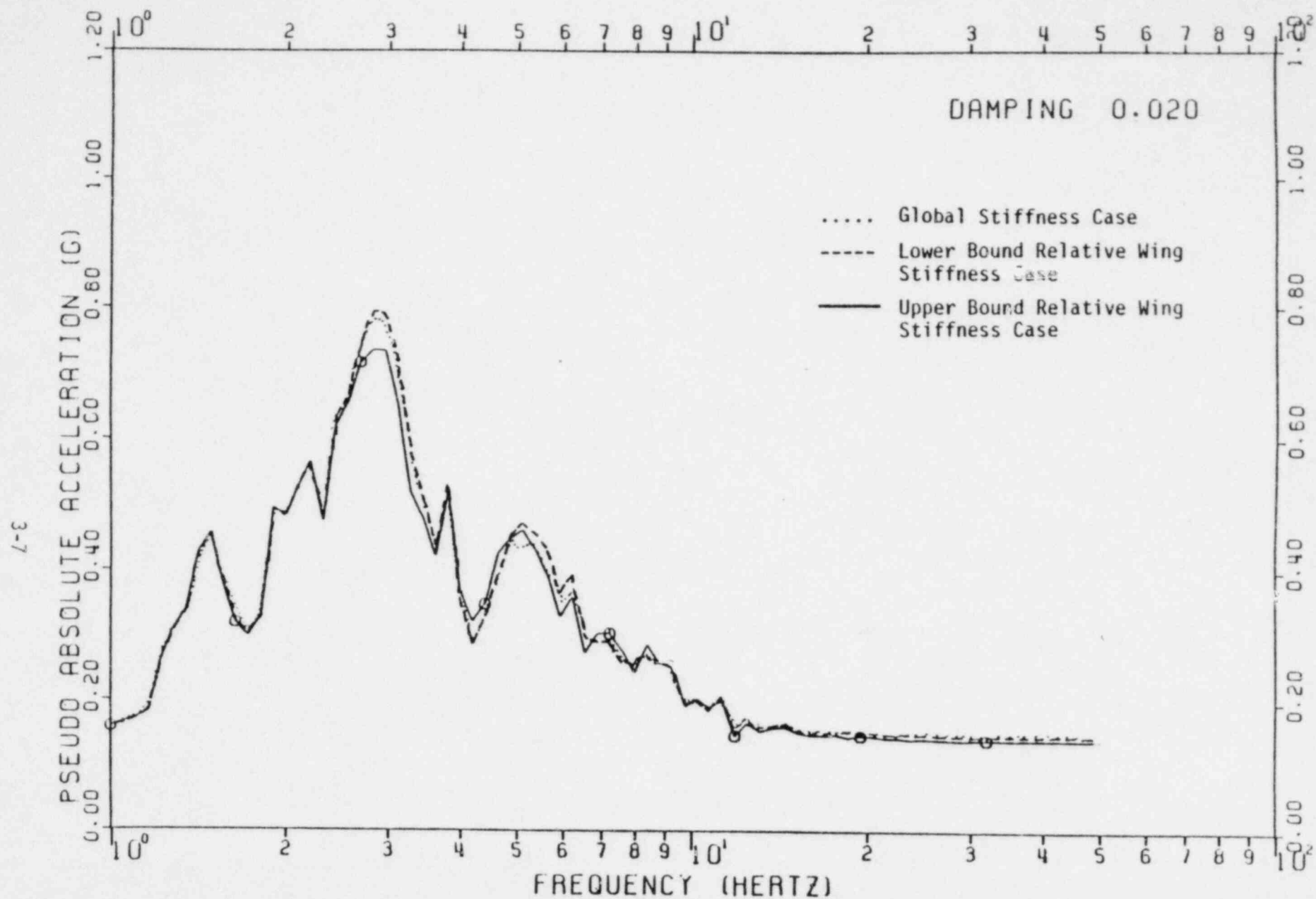


FIGURE 3-2. NORTH-SOUTH CONTROL TOWER RESPONSE DUE TO NORTH-SOUTH GROUND MOTION, ELEVATION 614 Ft.,
NODAL POINT 55

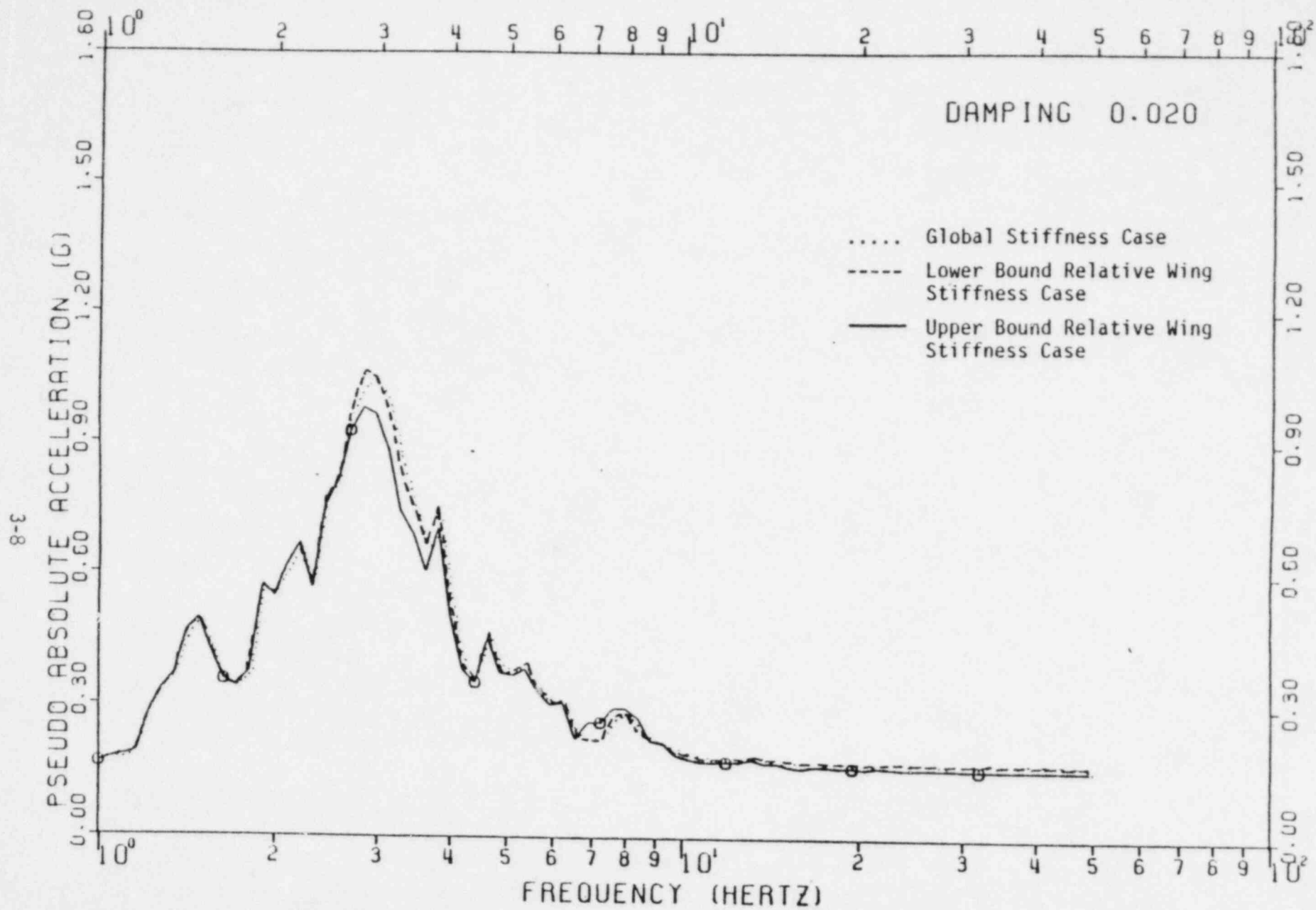


FIGURE 3-3. NORTH-SOUTH CONTROL TOWER RESPONSE DUE TO NORTH-SOUTH GROUND MOTION, ELEVATION 659 Ft.,
NODAL POINT 44

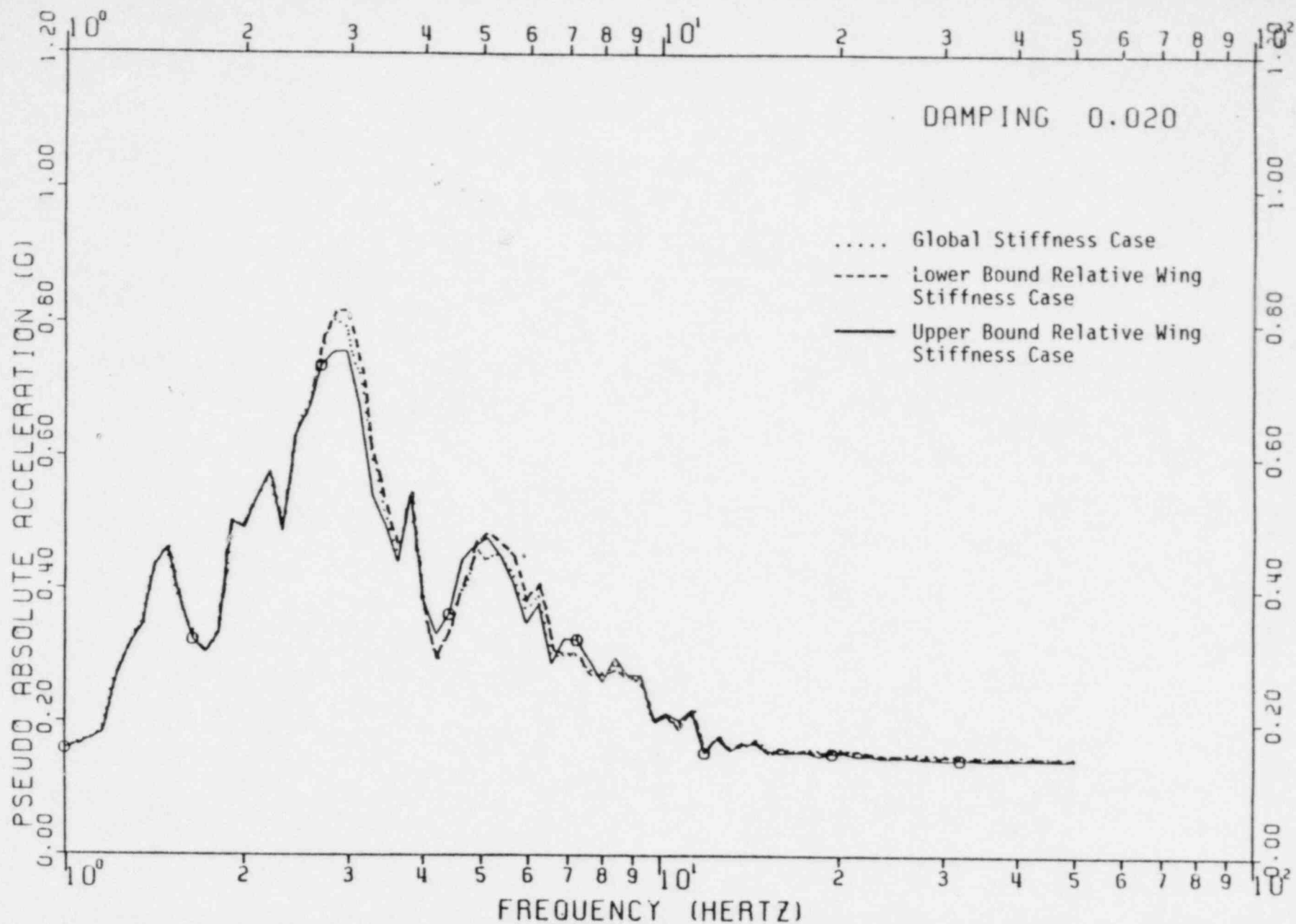


FIGURE 3-4. NORTH-SOUTH MAIN AUXILIARY BUILDING RESPONSE DUE TO NORTH-SOUTH GROUND MOTION, ELEVATION 614 Ft., NODAL POINT 28

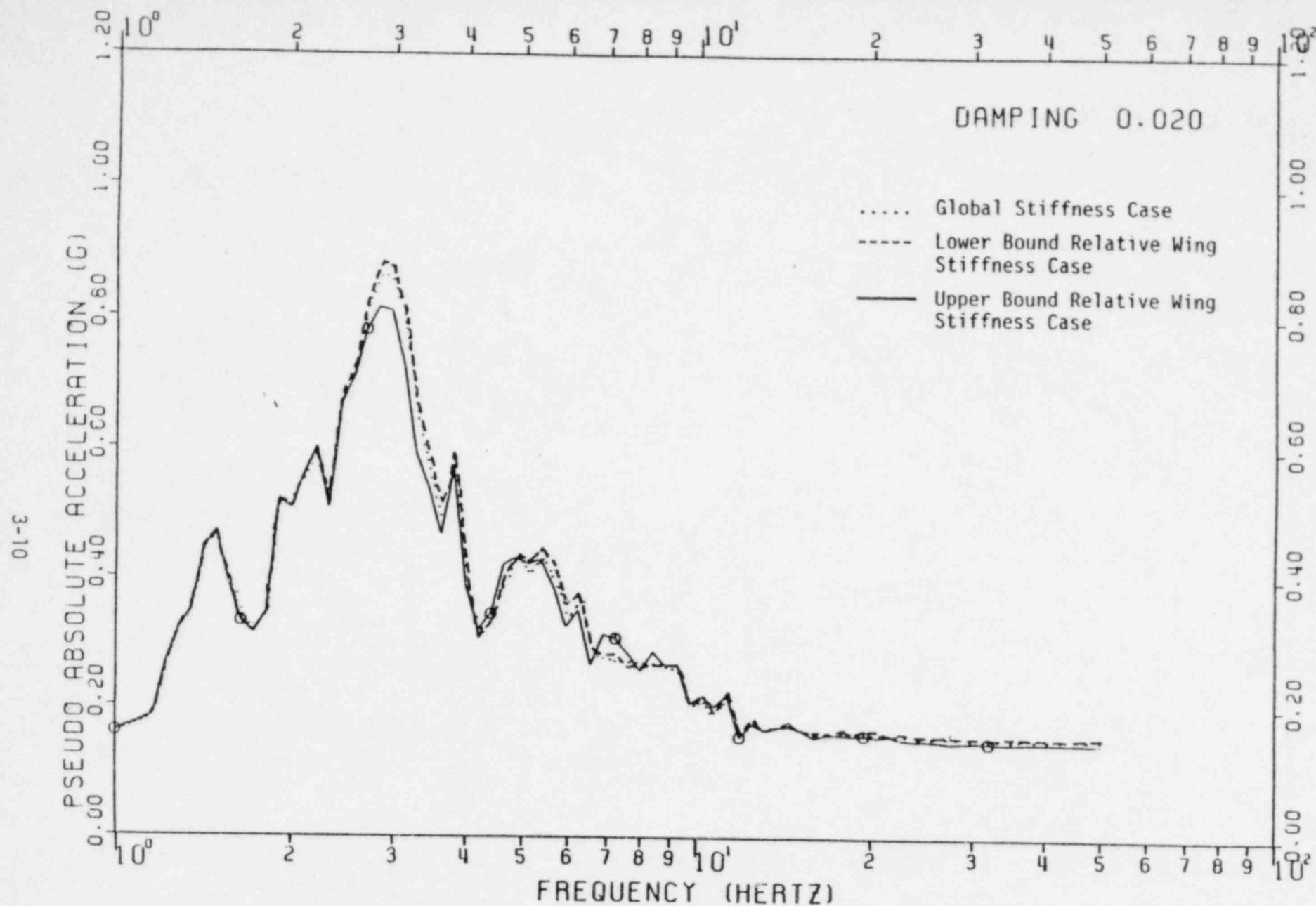


FIGURE 3-5. NORTH-SOUTH MAIN AUXILIARY BUILDING RESPONSE DUE TO NORTH-SOUTH GROUND MOTION, ELEVATION 628.5 Ft., NODAL POINT 24

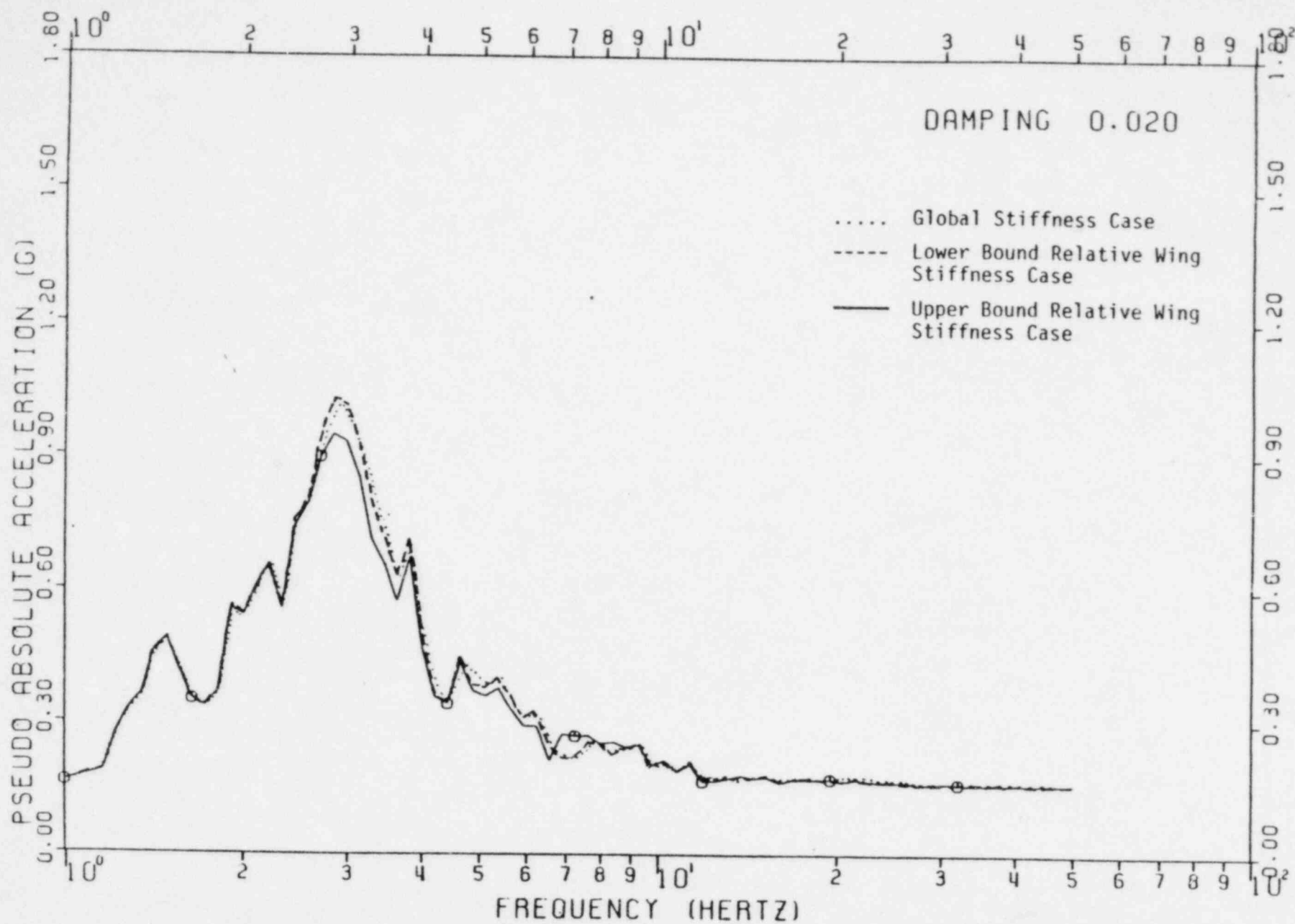


FIGURE 3-6. NORTH-SOUTH MAIN AUXILIARY BUILDING RESPONSE DUE TO NORTH-SOUTH GROUND MOTION, ELEVATION 659 Ft., NODAL POINT 10

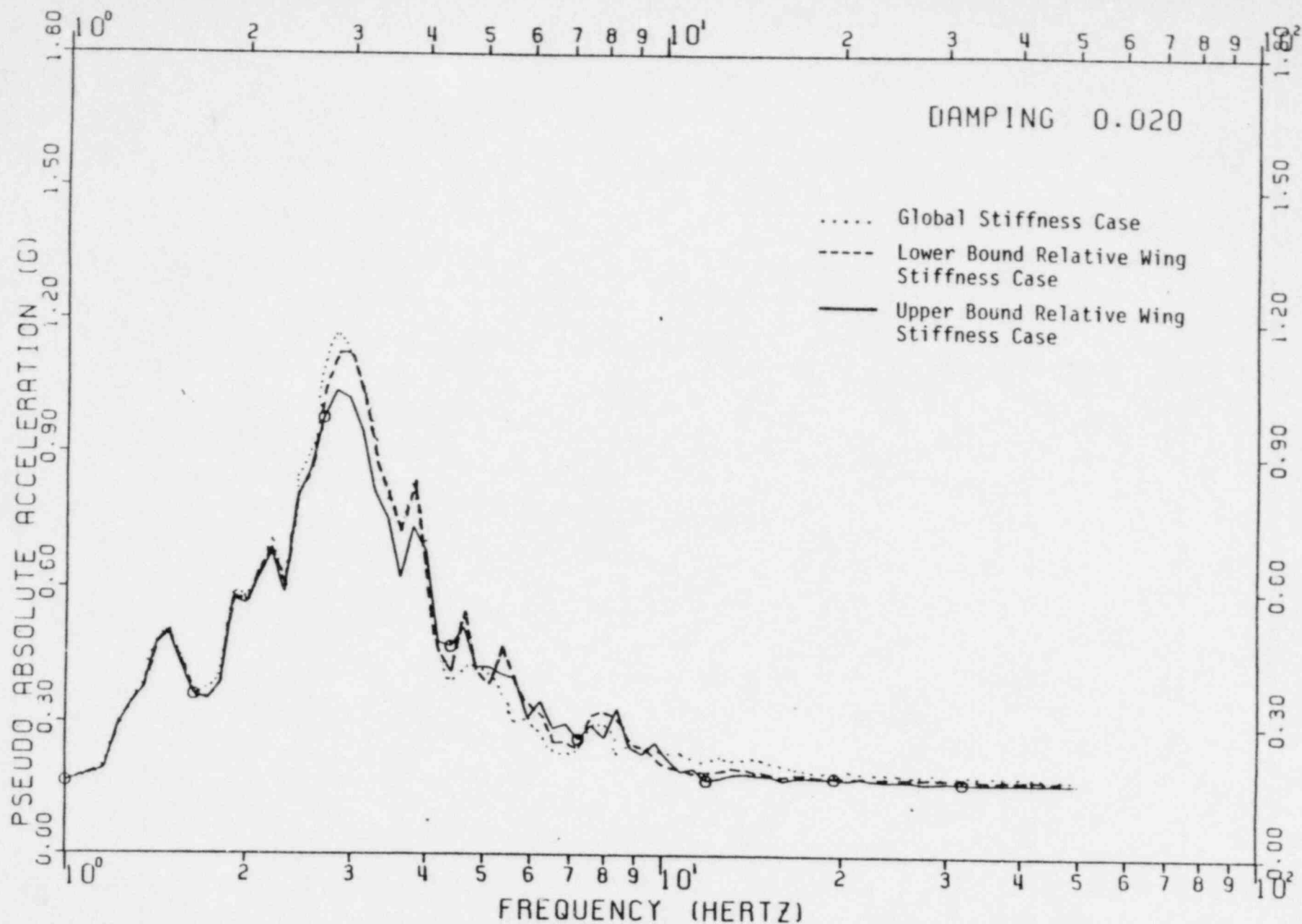


FIGURE 3-7. NORTH-SOUTH EAST ELECTRICAL PENETRATION WING RESPONSE DUE TO NORTH-SOUTH GROUND MOTION, ELEVATION 642.6 Ft., NODAL POINT 159

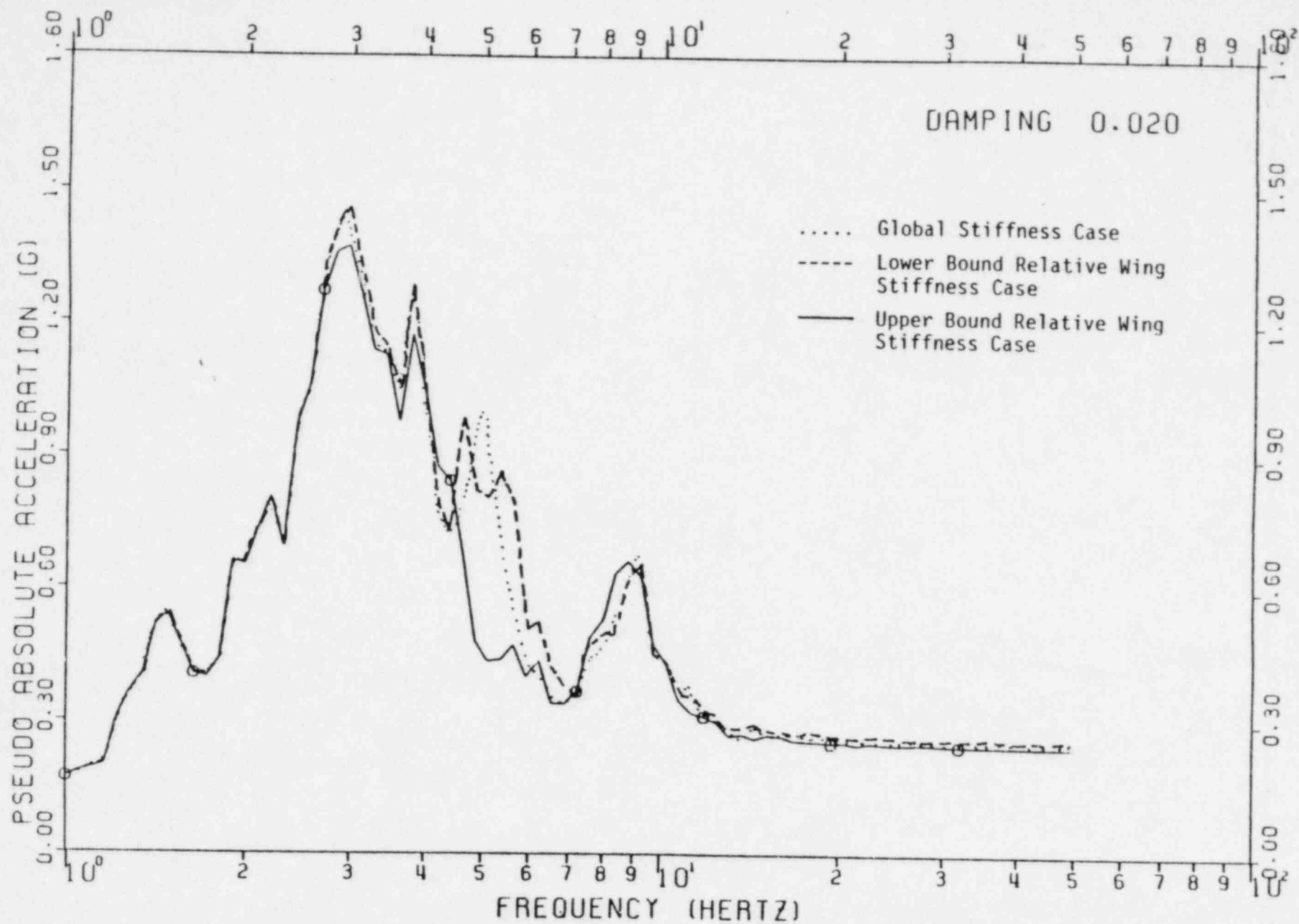


FIGURE 3-8. NORTH-SOUTH EAST ELECTRICAL PENETRATION WING RESPONSE DUE TO NORTH-SOUTH GROUND MOTION, ELEVATION 674.50 Ft., NODAL POINT 156

4. SUMMARY AND CONCLUSIONS

A parametric study has been conducted to evaluate the importance of developing discrete soil springs for use beneath the electrical penetration wings of the Midland Auxiliary Building mathematical model. Three cases were studied. The first case corresponded to a global stiffness case where soil impedances were developed based on the global foundation geometry of the auxiliary building complex and were attached to the mathematical model at a single location (i.e. zero relative stiffness was placed under each wing). The second case was defined as a lower bound relative wing stiffness case. This procedure minimized the relative soil stiffness beneath the wings and represents a realistic lower bound on the relative soil stiffnesses which are beneath the electrical penetration wings. Discrete soil springs were modeled under both the wings areas and main auxiliary/control tower for this case. The final case studied was defined as an upper bound relative wing stiffness case. The intent of this case was to maximize the relative soil stiffness under the wings and be an upper bound on the relative soil stiffnesses beneath the wing areas. Care was taken when developing cases two and three to maintain the same global stiffness and center of rotation as defined by the global stiffness case.

Response of the structure under N-S excitation was developed for each of the three cases. Results were obtained for this direction only since it represents the greatest flexibility in the electrical penetration wings and the maximum differences in response for the different cases would be expected for ground motion in this direction. In-structure floor response spectra, peak relative displacements, and peak absolute accelerations were developed for typical locations in the structure. Results showed that for all the locations studied, the floor response spectra, accelerations, and displacements were virtually identical. These results indicate that the base mat of the structure is translating and rotating as a rigid body. Therefore, it does not make much difference

how the soil is modeled in the analysis, so long as it is done consistently. The lower bound relative wing stiffness and global stiffness cases predict slightly more conservative spectral accelerations, zero-period accelerations, and displacements than the upper bound relative wing stiffness case. Therefore, it is recommended that the lower bound wing stiffness case be used for development of inertial loadings for determining moment and shear distributions in the structure. Either the lower bound relative stiffness or the global stiffness case should be used to determine in-structure floor response spectra.

REFERENCES

1. Bechtel submittal to WRC, "Auxiliary Building Seismic Model Revision 3 for Midland Plant Units 1 and 2 Consumers Power Company", September 28, 1981.
2. Kennedy, R. P., "Seismic Testimony for Midland Hearing", Nuclear Regulatory Commission, Docket No. 50-329 OL and OM, 50-330 OL and OM, Consumers Power Company, Midland Plant Units 1 and 2, December 14, 1981.
3. Richard, F. E., Hall, J. R. and R. A. Woods, Vibrations of Soils and Foundations, Prentice-Hall, Inc., New Jersey, 1970.
4. Wong, H. L. and J. E. Luco, "Soil-Structure Interaction: A Linear Continuum Mechanics Approach (CLASSI), Report, CE, Department of Civil Engineering, University of Southern California, Los Angeles, California, 1980.
5. Veletsos, A. S., and Y. T. Wei, "Lateral and Rocking Vibration of Footings", Journal of the Soil Mechanics and Foundations Division, Proceedings of ASCE, SM9, September, 1971, pp. 1227-1248.
6. Kausel, E., and R. Ushijima, "Vertical and Torsional Stiffness of Cylindrical Footings", Massachusetts Institute of Technology, Research Report R79-6, February, 1979.
7. Luco, J. E., and R. A. Westmann, "Dynamic Response of Circular Footings", Journal of the Engineering Mechanics Division, Proceedings of ASCE, EM5, October, 1971, pp. 1381-1395.
8. Johnson, J. J., "MODSAP-A Modified Version of the Structural Analysis Program SAP IV for the Static and Dynamic Response of Linear and Localized Nonlinear Structures", GA-A14006, UC-77, June, 1976.
9. Tsai, N. C., "Modal Damping for Soil-Structure Interaction", Journal of Engineering Mechanics Division, ASCE, Vol. 100, No. EM2, pp. 323-341, April, 1974.
10. Johnson, J. J., Letter to Dr. Thiru Thiruvengadam, Consumers Power Company, 1945 West Parnall Road, Jackson, Michigan, "Final Spectral Acceleration Values, Original Ground Surface and Top of Fill Site Specific Spectra Midland Site", January 27, 1982.
11. Levine, E. N., Letter to Dr. Thiru Thiruvengadam, Consumers Power Company, 1945 West Parnall Road, Jackson, Michigan, "Final Spectral Acceleration Values, Original Ground Surface and Top of Fill Site Specific Spectra Midland Site", January 27, 1982.

APPENDIX A

BACKUP CALCULATIONS FOR DEVELOPMENT OF LOWER AND UPPER
BOUND RELATIVE WING STIFFNESS CASES

Calculation of Actual Soil Springs for Use in Modern Aux. Bldg. Model

Upper and lower bound spring stiffnesses under the electrical penetration wings are desired in order to evaluate the effect of these different stiffnesses on the response of the aux. bldg. model. The following approach gives conservative lower \uparrow upper bounds on this stiffness.

Lower Bound

Steps:

1. Calculate global spring stiffnesses for the aux. bldg + electrical penetrations wing areas considered together.
2. Proportion the stiffnesses for E-W, N-S, + vertical translation under the electrical penetration wings out from the global stiffnesses determined in 1 above on the basis of contributory areas. These would be lower bound numbers since the actual spring impedances would be expected to be larger because this assumption assumes no independence of the wing foundations.
3. Ignore local torsional springs and rocking about the N-S axis under the electrical penetration wings.
4. For rocking about local E-W axes under the wings assume the following:

TITLE _____

BY RHK DATE 11/9/82

CHKD. BY PSH DATE 3/1/82



STRUCTURAL
MECHANICS
ASSOCIATES
A Calif. Corp.

PAGE 50 OF _____ Job No. _____

COMMENTS Upper + Lower

Bound Stiffness

$$a) \quad K_p(\text{lower bound}) = K_p^*(\text{Elect. Pen. Only})$$

$$\therefore K_p(\text{lower bound}) = K_p^*(\text{Elect. Pen. Only}) \quad K_p^*(\text{Elect. Pen. Only})$$

where: K_p^*, K_v^* are the elastic half space stiffnesses obtained by considering only the electrical penetration wings and ignoring the rest of the structure

$K_v(\text{lower bound})$ - defined by 2 above



Global Best Estimate Embedded Springs were previously developed (p. 28). These springs are calculated based on the assumption that the entire structure base mat acts as a single foundation. From p. 28 global stiffnesses are:

$$X \quad K_{N-S} = 3.56 \cdot 10^6 \text{ K/ft}$$

$$Y \quad K_{E-W} = 3.70 \cdot 10^6 \text{ K/ft}$$

$$K_{\text{vert}} = 3.97 \cdot 10^6 \text{ K/ft}$$

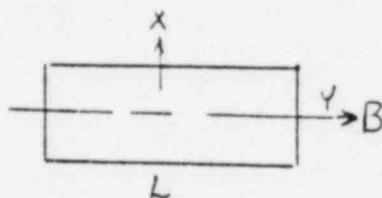
$$\text{about } Y \quad K_{\text{about}} = 6.53 \cdot 10^{10} \text{ K-ft/rad}$$

$$\text{about } X \quad K_{\text{about}} = 3.48 \cdot 10^{10} \text{ K-ft/rad}$$

$$K_{\theta} = 4.21 \cdot 10^{10} \text{ K-ft/rad}$$

Lower Bound Wing Stiffness

Idealized Representation of Electrical Penetration wings



See discussion on p. 53-53A for B, L

For N-S Motion

$$B = 26.1' \quad L = 53.3' \quad \frac{B}{L} = 0.49 \quad \beta_1 \approx 0.44 \quad p. 9$$

For E-W Motion

$$\frac{B}{L} = \frac{53.3}{26.1} = 2.04 \quad \beta_2 \approx 2.22 \quad p. 9$$

For a halfspace:
 (Assume same coeff.
 as determined for
 global solution for
 an effect)

$$K_2 = \frac{G}{1-\nu} \beta_2 \sqrt{A} K_4; \quad K_4 = \frac{G}{1-\nu} \beta_4 B^2 L k_2$$

$$\therefore \frac{K_4}{K_2} = \frac{k_2 \beta_4 B^2 L}{k_4 \beta_2 \sqrt{A}} = \frac{0.44 (26.1)^2 (53.3) (0.72)}{2.22 \sqrt{1592}} \cdot \frac{0.68}{0.68} = 204$$

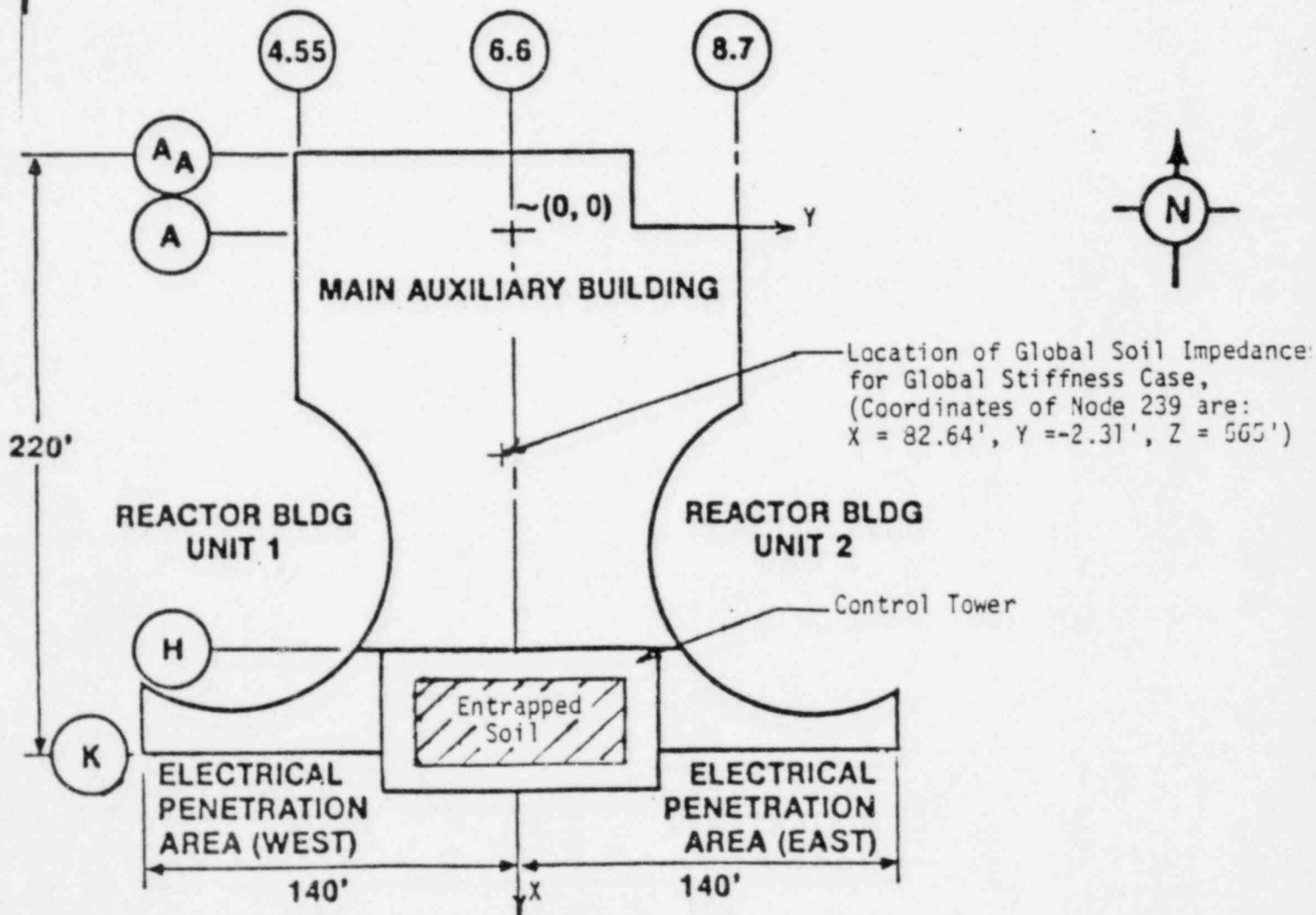
$$\therefore K_{\phi} (\text{lower bound}) = 204 K_2 (\text{lower bound})$$

$$\text{From p. 17} \quad K_2 = 0.68; \quad K_4 = 0.72$$



Centroidal Location for Aux. Bldg. Complex

As the diagram below shows the Aux. Bldg. complex consists of the main aux. bldg., the control tower, and the east and west electrical penetration wings. The foundation of the control tower consists of drilled shafts with a large mass of entrapped soil contained within them. In developing the global soil stiffness case (i.e. the soil impedances are calculated based on the overall foundation geometry) this entrapped soil was considered to move integrally with the foundation for horizontal translation dot and torsional dot. For rocking dot and vertical translation the foundation was assumed to move independently of the soil. As a consequence of this slightly different centroidal locations were obtained for translation/torsion dot and rocking/vertical dot. These were developed previously p. 0 to 42 but are presented here for review.



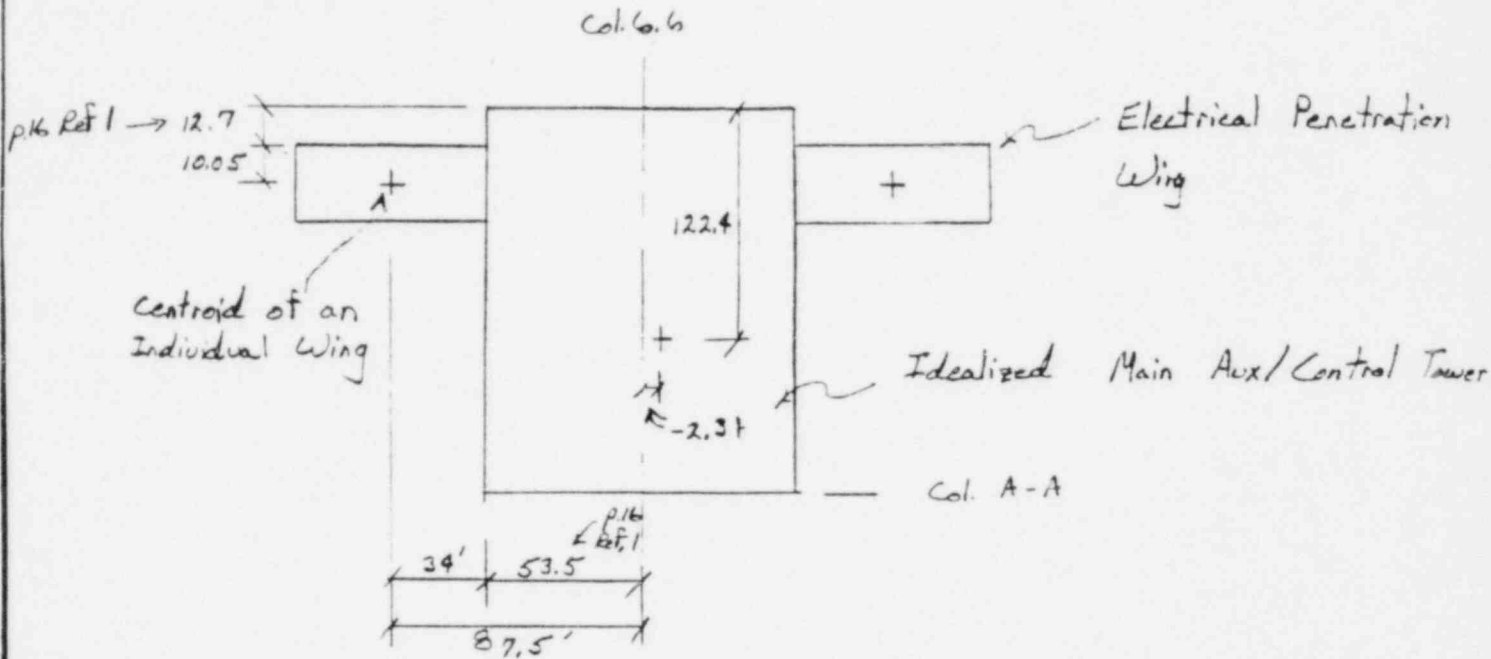
TITLE _____
 BY RHK DATE 1/20/82
 CHKD. BY PSH DATE 3/1/82



STRUCTURAL
 MECHANICS
 ASSOCIATES
 A CALIF. CORP.

PAGE 526 OF _____ Job No. 5
 COMMENTS Correction for
offsets

Centroidal Locations for Global Stiffness Case
Rocking + Vertical Def



Rocking / Vertical

$$A = 22940 + 4847 + 2(1392) = 30570 \text{ ft}^2$$

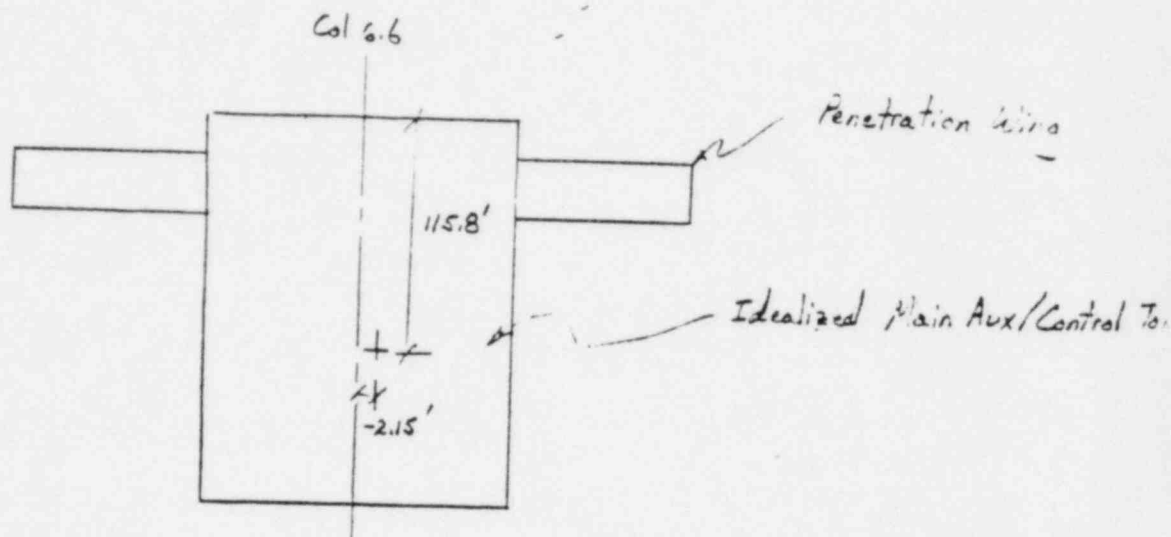
$$\bar{X} = \frac{132.3(27727) + 22.75(2)(1392)}{30570} = 122.4 \text{ ft.}$$

$$\bar{Y} = \frac{-2.54(27726)}{30570} = -2.31 \text{ ft.}$$

Numbers presented above are from p.c. 642 of
 S.S.I. Calc. for Aux. Eddy.

Centroidal Locations for Global Stiffness Case

Horiz. Translation + Torsional Load

Horiz Translation / Torsion

$$A = 30121 + 2(1392) = 32,905 \text{ ft}^2$$

$$\bar{X} = \frac{30121(124.4) + 2(1392)(22.75)}{32905} = 115.8'$$

$$\bar{Y} = \frac{30121(-2.25)}{32905} = -2.15'$$

Number presented above are from p. 0 to 42 of CSI
Calc for Horiz. Elns.

Major Base Elevations at Horiz. Elns. Complex

Elect. Penetration Wings \approx Elev. 573'

Main Aux/Control Tower \approx Elev. 565'

Difference in elevations is 8 ft.

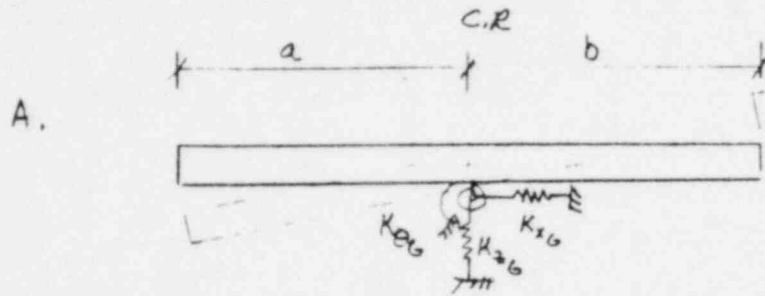
TITLE _____

BY: RHK DATE 11/25/82CHKD. BY: WJH DATE 3/1/82STRUCTURAL
MECHANICS
ASSOCIATES
A Calif. Corp.PAGE 526 OF _____ Job No. _____

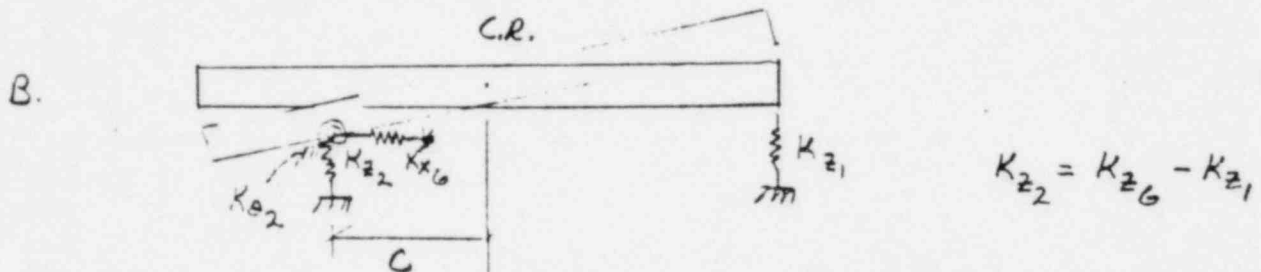
COMMENTS _____

Correction of Soil Impedances Beneath Main Aux/Control Tower

Soil Impedances are developed for the lower bound + upper bound wing stiffness cases. These solutions involve placing discrete springs beneath the wing areas in order to model the soil. However, in making comparisons with the global stiffness case, it is necessary to adjust the magnitude and centroidal location of the soil impedances beneath the main auxiliary/control tower portion of the building in order to maintain the same overall model characteristics which were found for the global stiffness case. This procedure for maintaining the same stiffness + center of rotation is developed for a 2 dimensional model on the next page. It then is expanded for the lower bound wing stiffness case.



Suppose we distribute K_{26} as follows and want to keep the same global center of rotation.



To locate the distance c , give model B a unit displacement Δ_1 downward and sum moments about the C.R.

$$\Delta_1 K_{22} c = \Delta_1 K_{21} b$$

$$c = \frac{K_{21} b}{K_{22}}$$

To calculate the correct moment K_{θ_2} , two steps must be followed:

1. Give model A a unit rotation θ_1 and calculate resisting moment at C.R.

$$M_{C.R.} = K_{\theta_6} \cdot \theta_1$$

2. Give model B a unit rotation and solve for M_{θ_2} such that equilibrium is obtained with $M_{C.R.}$.

For model B
$$M_{C.R.} = M_{\theta_2} + (c\theta) K_{22} c + K_{21} (b\theta) c$$

$$M_{\theta_2} = K_{\theta_2} \cdot \theta_1$$

TITLE _____
 BY RHK DATE 1/21/82
 CHKD. BY ZSH DATE 3/1/82



STRUCTURAL
 MECHANICS
 ASSOCIATES
 A CALIF. CORP.

PAGE 52E OF _____ Job No. _____
 COMMENTS Correction for
Effects

$$M_{\theta_2} = M_{c.r} - [c^2 K_{z_2} + b^2 K_{z_1}] \theta_1$$

$$K_{\theta_2} = K_{\theta_6} - \left[\left(\frac{K_{z_1}}{K_{z_2}} \right)^2 K_{z_2} + K_{z_1} \right] b^2$$

$$K_{\theta_2} = K_{\theta_6} - K_{z_1} \left[\frac{K_{z_1}}{K_{z_2}} + 1 \right] b^2$$

Correction of Global Stiffness at Node 239

Using p. 51, 52

$$N-S \quad K_{x_{239}} = 3.56 \cdot 10^6 - \frac{1392(2)}{32905} (3.56 \cdot 10^6) = 3.26 \cdot 10^6 \text{ K/ft}$$

$$E-W \quad K_{y_{239}} = 3.70 \cdot 10^6 \left(1 - \frac{1392(2)}{32905} \right) = 3.38 \cdot 10^6 \text{ K/ft}$$

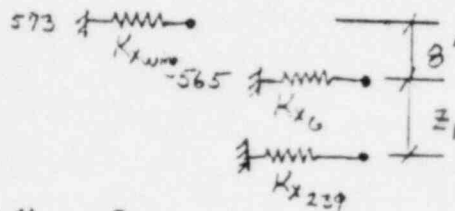
$$\text{Vert} \quad K_{z_{239}} = 3.97 \cdot 10^6 \left(1 - \frac{1392(2)}{30570} \right) = 3.61 \cdot 10^6 \text{ K/ft}$$

Calculate New Coordinate Locations For Node 239

The procedure shown on p. 520, 52E gives a deterministic answer when only 2 dimensions are considered in locating the location of the new spring centroid. However, when three dimensions are considered it turns out that you end up with 2 equations and one unknown for each of the three coordinates required. A best fit coordinate will be determined in each direction by solving each equation for the unknown dimension and averaging the results for the Y + Z directions. In the X direction the difference between the coordinates obtained from $\Sigma M_z + \Sigma M_y$ directions is the largest. In this direction the X coordinate associated with rocking in the N-S direction will be used since this is the direction of particular interest in the Jura Alda model.



Lower Bound Wire Stiffness Case
Z Coordinate



$$\sum M_y = 0$$

$$z_1 K_{x239} - K_{xw}(z) = 0$$

$$z_1 = \frac{8 K_{xw}}{K_{x239}} = \frac{8(0.30 \cdot 10^6)}{3.26 \cdot 10^6}$$

$$z_1 = 0.74' \text{ below elev. } 565'$$

Similarly

$$\sum M_x = 0$$

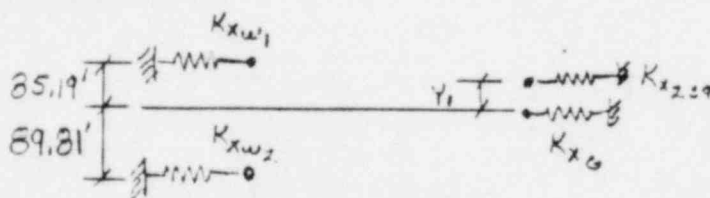
$$z_2 K_{y239} - K_{yw}(z) = 0$$

$$z_2 = \frac{8 K_{yw}}{K_{y239}} = \frac{8(0.32 \cdot 10^6)}{3.38 \cdot 10^6}$$

$$z_2 = 0.76' \text{ below elev. } 565'$$

Use $z = 0.75' \text{ below elev. } 565'$

Y Coordinate



$$K_{xw1} = K_{xw2}$$

$$\sum M_z = 0$$

$$K_{x239} y_1 + (85.35 - 89.65) K_{xw1} = 0 \quad P.52B$$

$$y_1 = \frac{4.30 K_{xw}}{K_{x239}}$$

$$y_1 = \frac{4.30 (0.15 \cdot 10^6)}{3.26}$$

$$y_1 = 0.20$$

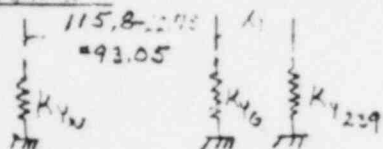
$$\sum M_x = 0$$

$$K_{z239} y_2 + 85.19 K_{zw1}$$

$$- 89.81 K_{zw2} = 0 \quad P.52C$$

$$y_2 = \frac{4.62 K_{zw1}}{K_{z239}} = \frac{4.62 (0.15 \cdot 10^6)}{3.41 \cdot 10^6}$$

$$y_2 = 0.23' \quad \text{Use } y_1 = 0.21' \text{ at}$$

X Coordinate

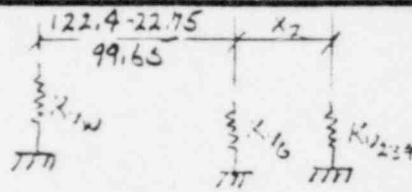
$$\sum M_z = 0$$

$$K_{YW}(93.05) - K_{Y239}X_1 = 0$$

$$X_1 = \frac{93.05 K_{YW}}{K_{Y239}}$$

$$X_1 = \frac{93.05(0.32 \cdot 10^6)}{3.38 \cdot 10^6}$$

$$X_1 = 8.81'$$



$$\sum M_y = 0$$

$$K_{YW}99.65 - K_{Y239}X_2 = 0$$

$$X_2 = \frac{99.65 K_{YW}}{K_{Y239}}$$

$$X_2 = \frac{99.65(0.36)}{3.61}$$

$$X_2 = 9.94'$$

Distances are in feet

North of current location

Use $X_2 = 9.94$ ft since we are worried about rotations in this direction.Correct Rotational Springs at these locations

1. Apply Unit Rotation at old node 239 location about the N-S Axis.

Define $M_{\theta_{xx}}$ as moment we want to determine $M_{\theta_{xx}}$ - moment at C.R. due to original global rot. stiffnesses

$$M_{\theta_{xx}} = M_{\theta_{xx}} + \frac{1}{2}K_{2w} [85.19^2 + 89.81^2] + K_{239} (0.23)^2 + K_{YW} [8]^2 + K_{Y239} [0.76]^2$$

(122.4, -2.31)

Solving for $K_{\theta_{xx}}$

$$K_{\theta_{xx}} = K_{\theta_{xx}} - \frac{1}{2}K_{2w} [85.19^2 + 89.81^2] - K_{239} (0.23)^2 - K_{YW} 8^2 - K_{Y239} [0.76]^2$$

$$K_{\theta_{xx}} = 3.48 \cdot 10^{10} - \frac{1}{2} [15325] 0.36 \cdot 10^6 - 3.61 \cdot 10^6 (0.23)^2 - 3.38 \cdot 10^6 (0.76)^2$$

$$K_{\theta_{xx}} = 3.20 \cdot 10^{10} \text{ K-in/rad}$$



2. Apply unit rotation at old node 229 location about the EW Axes
 Solve for $K_{\phi YY}$

$$M_{CEYY} = M_{\phi YY} + \sum M_{\phi YY \text{ wings}} + K_{Z22} \theta_2 [99.65]^2 + K_{Z229} [9.94]^2 \theta_2 \\ + K_{XW} [2]^2 + K_{X239} (0.74)^2 \theta_2$$

$$K_{\phi YY} = K_{\phi YYG} - \sum K_{\phi YY \text{ wings}} - 99.65^2 K_{Z22} - 9.94^2 K_{Z229} \\ - 2^2 K_{XW} - 0.74^2 K_{X239}$$

$$K_{\phi YY} = 4.63 \cdot 10^{10} - 2(36.72 \cdot 10^6) - 99.65^2 (0.36 \cdot 10^6) - 9.94^2 (3.61 \cdot 10^6) \\ - 64 (0.30 \cdot 10^6) - 0.74^2 (3.26 \cdot 10^6)$$

$$K_{\phi YY} = 4.23 \cdot 10^{10} \frac{\text{Kft}}{\text{rad}}$$

3. Apply unit rotation at old node 239 location about vertical axis:

$$M_{CEZZ} = M_{\phi ZZ} + [K_{XW1} [35.35^2 + 89.65^2] + K_{X239} (0.20)^2 \\ + K_{YW} [93.05]^2 + K_{Y239} [8.81]^2] \theta_3$$

$$K_{\phi ZZ} = K_{\phi ZZG} - 93.05^2 K_{YW} - 8.81^2 K_{Y239} - 0.20^2 K_{X239} \\ - [35.35^2 + 89.65^2] K_{XW1}$$

$$K_{\phi ZZ} = 4.21 \cdot 10^{10} - 93.05^2 (0.32 \cdot 10^6) - 8.81^2 (3.38 \cdot 10^6) - 0 \\ - [35.35^2 + 89.65^2] (0.30 \cdot 10^6) \left(\frac{1}{2}\right)$$

$$K_{\phi ZZ} = 3.68 \cdot 10^{10} \frac{\text{Kft}}{\text{rad}}$$

TITLE _____

BY RHK DATE 1/19/82CHKD. BY JEH DATE 3/1/82

STRUCTURAL
MECHANICS
ASSOCIATES
A Calif. Corp.

PAGE 524 OF _____ Job No. _____

COMMENTS _____

Lower Bound Stiffnesses

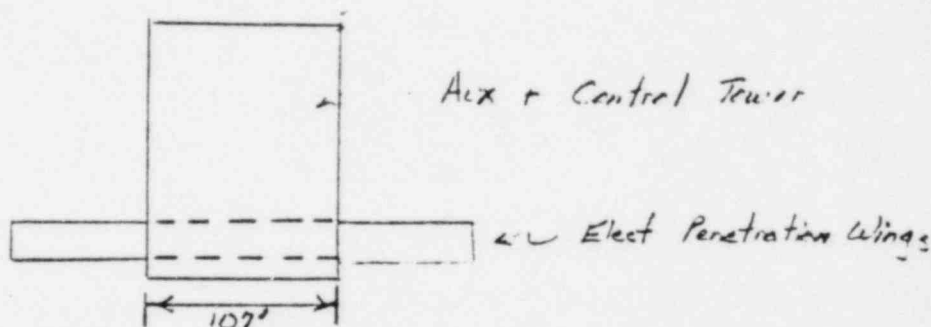
Area ratios, etc. are based on p. 89 Ref. 1,
x = N-S, y = E-W, z = Vert; ϕ_{yy} = rock about E-W

SMA Node #	Bechtel Node #	Local Wing Node Area (ft) ²	Total Global Spring Area (ft ²)	"Best" Estimate Soil
31,68	214 217	X 385	32905	$4.17 \cdot 10^4$
		Y 385	32905	$4.33 \cdot 10^4$
		Z 385	30570	$5.00 \cdot 10^4$
		ϕ_{yy}		$1.02 \cdot 10^7$
10,88	211 220	X 415	32905	$4.49 \cdot 10^4$
		Y 415	32905	$4.67 \cdot 10^4$
		Z 415	30570	$5.39 \cdot 10^4$
		ϕ_{yy}		$1.10 \cdot 10^7$
6,104	112 168	X 109.5	32905	$1.18 \cdot 10^4$
		Y 109.5	32905	$1.23 \cdot 10^4$
		Z 109.5	30570	$1.42 \cdot 10^4$
		ϕ_{yy}		$2.90 \cdot 10^6$
3,131	208 223	X 231.5	32905	$2.50 \cdot 10^4$
		Y 231.5	32905	$2.60 \cdot 10^4$
		Z 231.5	30570	$3.01 \cdot 10^4$
		ϕ_{yy}		$6.13 \cdot 10^6$
2,153	205 226	X 201.9	32905	$2.18 \cdot 10^4$
		Y 201.9	32905	$2.27 \cdot 10^4$
		Z 201.9	30570	$2.62 \cdot 10^4$
		ϕ_{yy}		$5.35 \cdot 10^6$
1,173	269 272	X 49.9	32905	$5.40 \cdot 10^3$
		Y 49.9	32905	$5.61 \cdot 10^3$
		Z 49.9	30570	$6.48 \cdot 10^3$
		ϕ_{yy}		$1.32 \cdot 10^6$
18	239	N-S X 3012.1	32905	$3.26 \cdot 10^6$
		E-W Y 2512.1	32905	$3.38 \cdot 10^6$
		Vert Z 27786.5	30570	$3.61 \cdot 10^6$
		ϕ_{xx}		$3.20 \cdot 10^{10}$
		ϕ_{yy}		$4.23 \cdot 10^{10}$
		ϕ_{zz}		$3.68 \cdot 10^{10}$

} See p. 52A - 52G

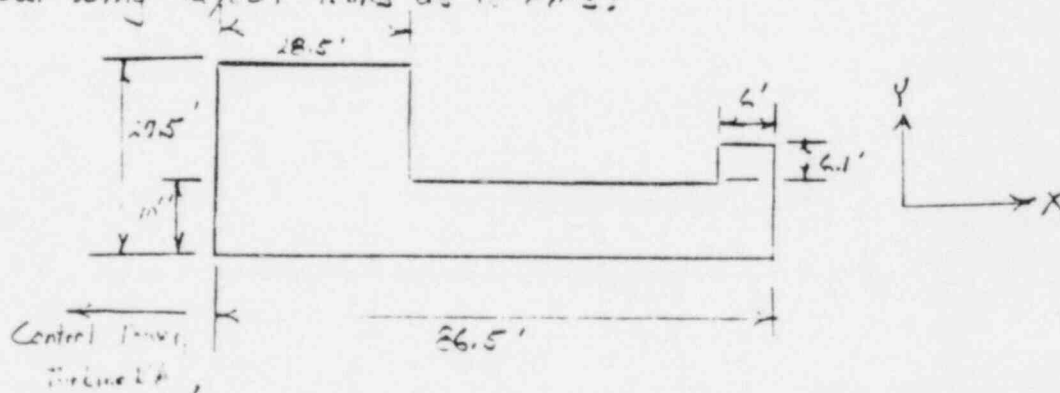
Upper Round Stiffness

The Aux. Bldg. in plan view looks approximately as follows:



The minimum possible ^{soil stress bulb} interaction which could occur when considering the electrical penetration wings and the Aux. Bldg together is shown above. This model would consider a single long foundation consisting of the two electrical penetration wings and a strip through the central tower equal in width to the electrical penetration wings. Obviously, the main aux/control tower would have greater effects ^{on the wing stiffness} than what we are assuming. However, our conservative assumption will give an upper bound solution for the wing stiffness.

The actual wing layout looks as follows:



Examination of this foundation indicates that most of the structure and inertia is heavily weighted towards the end of the wing closest to the central tower. This interaction ^{between the control tower and wings} could be substantial. Therefore the



idealized model of the wings chosen will be one which emphasizes a weighting of dimensions such that a short squat model of the wings is obtained.

For one wing;

$$A = 1392 \text{ ft}^2 \quad I_x = 931159 \text{ ft}^4 \quad I_y = 79304 \text{ ft}^4 \quad \text{Ref. p. 26}$$

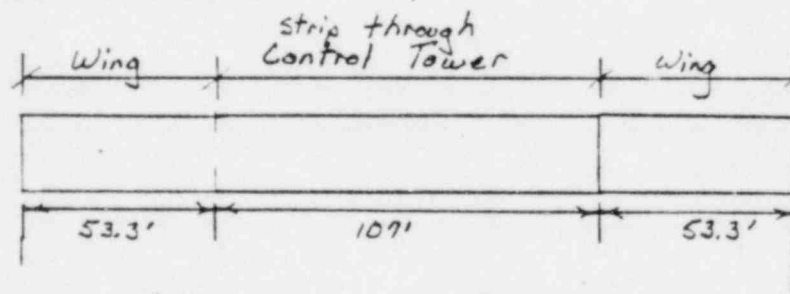
$$I = \frac{1}{12} b h^3 \quad A = b h \quad \therefore h = \sqrt{\frac{12I}{A}}$$

$$\text{For about X} \quad h = \sqrt{\frac{12(931159)}{1392}} = 89.6 \text{ ft} \quad b = \frac{1392}{89.6} = 15.5'$$

$$\text{For about Y} \quad h = \sqrt{\frac{12(79304)}{1392}} = 26.1 \text{ ft} \quad b = \frac{1392}{26.1} = 53.3'$$

In order to maximize interaction effects use $h = 26.1'$
 $b = 53.3'$ for both directions.

Idealized Foundation



$$A_T = 213.6(26.1) = 5575 \text{ ft}^2$$

E-W Translation, Vertical Translation

$$\frac{B}{L} = \frac{213.6}{26.1} = 8.18 \quad B_x \approx 1.14 \quad B_z \approx 2.17 \quad \text{p. 9}$$

N-S Translation, Rocking

$$\frac{B}{L} = \frac{1}{8.18} = 0.122 \quad B_x \approx 1.27 \quad B_y \approx 0.38 \quad \text{p. 9}$$

Halfspace Equations (Frequency Dependent)

$$K_x = k_1 2(1+\nu) G B_x \sqrt{A}$$

Use p. 28 - embedment factors

$$K_z = k_3 \frac{G}{1-\nu} B_z \sqrt{A}$$

Use p. 17 - k_1, k_2, k_3

$$K_p = k_2 \frac{G}{1-\nu} B_y L^2$$

Use from p. 68

$$G = 7100 \text{ Ksf}$$

Translation, Torsion

$$L = 2100 \text{ Ksf}$$

Rocking, Flexure

TITLE _____

BY RHK DATE 1/12/82CHKD. BY PSH DATE 3/1/82STRUCTURAL
MECHANICS
ASSOCIATES
A Calif. Corp.PAGE 54 OF 16 Job No. _____COMMENTS Upper RoundStiffnessesStiffnesses for each Wing

$$K_{xwing} = \frac{(1392) K_x \cdot F_{Ex}}{5575}$$

$$K_{ywing} = \frac{(1392) K_y \cdot F_{Ey}}{5575}$$

$$K_{zwing} = \frac{(1392) K_z \cdot F_{Ez}}{5575}$$

F_{Ex}, F_{Ey}, F_{Ez} = embedment factors for
Aux. Bldg + Electrical
Penetration wings

E-W

$$K_{ywing} = \frac{(1392)}{(5575)} (0.96) (1+0.42)(2)(7100)(1.14) \sqrt{5575} (1.10)$$

$$K_{ywing} = 4.53 \cdot 10^5 \text{ K/ft}$$

N-S

$$K_{xwing} = \frac{(1392)}{(5575)} (0.96) (1.42)(2)(7100)(1.27) \sqrt{5575} (1.11)$$

$$K_{xwing} = 5.09 \cdot 10^5 \text{ K/ft}$$

Vert

$$K_{ywing} = \frac{(1392)}{(5575)} (0.68) \left(\frac{26.1}{1-0.42} \right) (2.70) \sqrt{5575} (1.09)$$

$$K_{ywing} = 5.53 \cdot 10^5 \text{ K/ft}$$

Rock about
E-W

$$K_{\phi wing} = (0.72)(0.38) \left(\frac{2600}{1-0.42} \right) (26.1)^2 (213.6) (1.24) \left(\frac{1392}{5575} \right)$$

$$K_{\phi wing} = 1.83 \cdot 10^8 \text{ K-ft/rad.}$$

To obtain nodal spring stiffnesses proportion overall
wing stiffnesses by contributory area.

TITLE _____

BY RHK DATE 11/1/82

CHKD. BY ASH DATE 3/1/82



STRUCTURAL
MECHANICS
ASSOCIATES
A Calif. Corp.

PAGE 54A OF _____ Job No. _____

COMMENTS Upper Bound

Wing Stiffness

Upper Bound Stiffnesses

SMA Node #	Bechtel Node #	Local Wing Node Area (ft) ²	Total Wing Area (ft) ²	"Best" Estimate Soil
31,68	214	X Y Z A _{xy}	1392	1.41 · 10 ⁵
	217			1.25 · 10 ⁵ 1.53 · 10 ⁵ 5.06 · 10 ⁷
10,88	211	X Y Z A _{xy}	1392	1.52 · 10 ⁵
	220			1.35 · 10 ⁵ 1.65 · 10 ⁵ 5.46 · 10 ⁷
6,109	112	X Y Z A _{xy}	1392	4.00 · 10 ⁴
	168			3.56 · 10 ⁴ 4.35 · 10 ⁴ 1.44 · 10 ⁷
3,131	208	X Y Z A _{xy}	1392	8.47 · 10 ⁴
	223			7.53 · 10 ⁴ 9.20 · 10 ⁴ 3.04 · 10 ⁷
2,153	205	X Y Z A _{xy}	1392	7.38 · 10 ⁴
	226			6.57 · 10 ⁴ 8.02 · 10 ⁴ 2.65 · 10 ⁷
1,173	269	X Y Z A _{xy}	1392	1.82 · 10 ⁴
	272			1.62 · 10 ⁴ 1.98 · 10 ⁴ 6.56 · 10 ⁶
18	N-S E-W 239	X Y Z A _{xx} A _{yy} A _{zz}		2.54 · 10 ⁶
				2.79 · 10 ⁶ 2.86 · 10 ⁶ 2.62 · 10 ¹⁰ 3.05 · 10 ¹⁰ 2.39 · 10 ¹⁰

} See p. 55 to 56

To calculate node 239 X, Y, Z, subtract out wing stiffness from global embedded stiffnesses

TITLE _____
 BY RHK DATE 1/2/82
 CHKD. BY SSW DATE 3/1/82



STRUCTURAL
 MECHANICS
 ASSOCIATES
 A Calif. Corp.

PAGE 55 OF 18 Job No. _____
 COMMENTS Correction for
offset

Correction of Global Stiffness at Node 239 - Upper Round Case
 p. 51

$$N-S \quad K_{x239} = 3.56 \cdot 10^6 - 2(5.09 \cdot 10^5) = 2.54 \cdot 10^6 \text{ K/ft}$$

$$E-W \quad K_{y239} = 3.70 \cdot 10^6 - 2(4.53 \cdot 10^5) = 2.79 \cdot 10^6 \text{ K/ft}$$

$$Vert \quad K_{z239} = 3.97 \cdot 10^6 - 2(5.53 \cdot 10^5) = 2.86 \cdot 10^6 \text{ K/ft}$$

Calculation of New Coordinates for Node 239

Use procedure shown on p. 52E - 52F, see p. 52B, C for initial coordinate locations

Z Coordinate

$$Z_1 = \frac{8 K_{xw}}{K_{x239}}$$

$$Z_1 = \frac{8(1.02 \cdot 10^6)}{2.54 \cdot 10^6}$$

$$Z_1 = 3.21'$$

$$Z_2 = \frac{8 K_{yw}}{K_{y239}}$$

$$Z_2 = \frac{8(0.906)}{2.79}$$

$$Z_2 = 2.60' \quad \text{Use } Z_{ave} = 2.91'$$

Distances are in number of ft. below elevation 555'

Y Coordinate

$$Y_1 = \frac{4.30 K_{xw}}{K_{x239}}$$

$$Y_1 = \frac{4.30(0.509)}{2.54}$$

$$Y_1 = 0.86'$$

$$Y_2 = \frac{4.62 K_{zw}}{K_{z239}}$$

$$Y_2 = \frac{4.62(0.553)}{2.86}$$

$$Y_2 = 0.89 \quad \text{Use } Y_{ave} = 0.88'$$

Distances in number of feet, west of current location of translational springs

X Coordinate

$$X_1 = \frac{93.05 K_{yw}}{K_{y239}}$$

$$X_1 = \frac{93.05(0.906)}{2.79}$$

$$X_1 = 30.22 \text{ ft.}$$

$$X_2 = \frac{99.65 K_{zw}}{K_{z239}}$$

$$X_2 = \frac{99.65(1.11)}{2.86}$$

$$X_2 = 38.68 \text{ ft.}$$

Distances are in number of feet from current coordinate location

Use $X_2 = 38.68'$ since we are worried about rotations in

Rotation about X (N-S Axis)

$$K_{\phi_{xx}} = K_{\phi_{xxG}} - K_{\phi_{xw}} \left(\frac{1}{2} \right) [85.17^2 + 29.21^2] - K_{\phi_{23}} y_2^2 \\ - 8^2 K_{\phi_{w}} - K_{\phi_{23}} z_2^2$$

$$K_{\phi_{xx}} = 3.48 \cdot 10^{10} - \left(\frac{1}{2} \right) (1.11 \cdot 10^6) [85.17^2 + 29.21^2] - 2.86 \cdot 10^6 (2.89) \\ - 64 (0.906 \cdot 10^6) - (2.79 \cdot 10^5) (2.60)^2$$

$$K_{\phi_{xx}} = 2.62 \cdot 10^{10} \text{ K-ft/rad}$$

Rotation about Y (about E-W Axis)

$$K_{\phi_{yy}} = K_{\phi_{yyG}} - \sum K_{\phi_{yw}} - 99.65^2 K_{\phi_{w}} - x_2^2 K_{\phi_{23}} - 8^2 K_{\phi_{w}} - z_1^2 K_{\phi_{23}}$$

$$K_{\phi_{yy}} = 4.63 \cdot 10^{10} - 2 (1.83 \cdot 10^8) - 99.65^2 (1.11 \cdot 10^5) - (38.68^2) (2.86 \cdot 10^6) \\ - 64 (1.02 \cdot 10^6) - 3.21^2 (2.54 \cdot 10^6)$$

$$K_{\phi_{yy}} = 3.05 \cdot 10^{10} \text{ K-ft/rad}$$

Rotation about Z

$$K_{\phi_{zz}} = K_{\phi_{zzG}} - 93.05^2 K_{\phi_{w}} - x_1^2 K_{\phi_{23}} - \left(\frac{1}{2} \right) K_{\phi_{w}} [85.35^2 + 89.65^2] \\ - y_1^2 K_{\phi_{23}}$$

$$K_{\phi_{zz}} = 4.21 \cdot 10^{10} - (93.05)^2 (0.906 \cdot 10^6) - (30.22)^2 (2.79 \cdot 10^5) \\ - \frac{1}{2} [1.02 \cdot 10^6] [85.35^2 + 89.65^2] - (0.86)^2 (2.54 \cdot 10^6)$$

$$K_{\phi_{zz}} = 2.39 \cdot 10^{10} \text{ K-ft/rad}$$

TITLE _____

BY RHK DATE 1/21/82CHKD. BY JSH DATE 3/1/82
 STRUCTURAL
MECHANICS
ASSOCIATES
A Calif. Corp.
PAGE 57A OF 20 Job No. _____COMMENTS Calculation ofMSAP CoordinatesGlobal Stiffness Case Coordinates (ft)

Node	X	Y	Z
18	81.64	-2.31	565.0'

Lower Bound Wing Stiffness Case

From p.52E, 52F

Z shifts 0.75' down

Y shifts 0.21' West

X shifts 1.94' North

w.r.t. global stiffness case
node 18 location

Node	X	Y	Z
18	71.70	-2.52	564.25

Upper Bound Wing Stiffness Case

From p.55

Z shifts 2.91' down

Y shifts 0.88' West

X shifts 38.62' North

w.r.t. global stiffness case
node 18 location

Node	X	Y	Z
18	42.96	-3.19	562.09

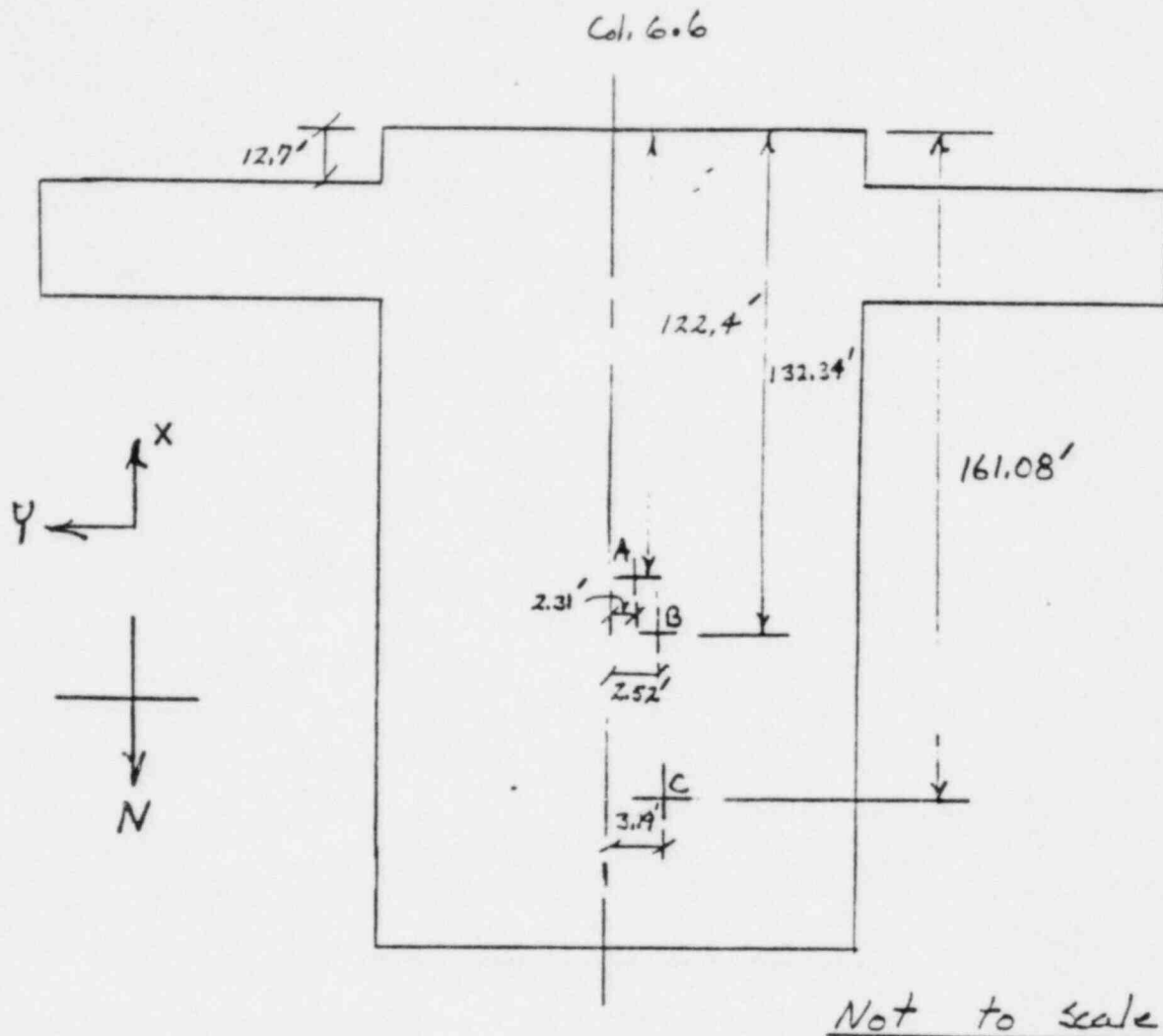
TITLE _____

BY RAK DATE 2/15/82CHKD. BY PSH DATE 3/1/82

STRUCTURAL
MECHANICS
ASSOCIATES
A CALIF. CORP.

PAGE 57B OF _____ Job No. _____

COMMENTS _____



Idealized Plan View of Aux. Bldg. Foundation

Location

Comment

- A - All soil impedances lumped at the base mat centroid in the Aux. Bldg. mathematical model
- B - Location of Aux. Bldg./Control Tower soil impedance when lower bound relative wing spring stiffnesses are used
- C - Location of Aux. Bldg./Control Tower soil impedance when upper bound relative wing spring stiffnesses are used

Figure - Schematic Representation of Aux. Bldg. Foundation showing Shifting of Location of Soil Impedance Under Main Aux./Control Tower When Soil Stiffness is Assigned to Electrical Penetration Wings

TITLE _____
BY BHK DATE 1/25/82
CHKD. BY DSH DATE 3/1/82



STRUCTURAL
MECHANICS
ASSOCIATES
A Calif. Corp.

PAGE 58 OF _____ Job No. _____
COMMENTS Tabulate Upper
and Lower Load Cases

Total Embedded Spring Stiffnesses Under An Individual Penetration Along

Direction	Lower Load	Upper Load	Ratio U/L
E-W Tran	$0.16 \cdot 10^6 \text{ K/ft}$	$0.45 \cdot 10^5 \text{ K/ft}$	2.81
N-S Tran	$0.15 \cdot 10^6 \text{ K/ft}$	$0.51 \cdot 10^6 \text{ K/ft}$	3.40
Vert Tran	$0.12 \cdot 10^6 \text{ K/ft}$	$0.55 \cdot 10^6 \text{ K/ft}$	3.06
Rock about EW	$3.67 \cdot 10^7 \frac{\text{K-ft}}{\text{rad}}$	$1.83 \cdot 10^8 \frac{\text{K-ft}}{\text{rad}}$	4.98
Rock about NS	0.	0.	—
Torsion	0.	0.	—



Node 18⁽²³⁹⁾ mass for this problem was calculated with the coordinates at the original model. (i.e. $X_G = 81.64$, $Y_G = -2.31$, $Z_G = 565.00$). For the Modsap analyses, whenever node 18 is shifted due to breaking contributory wing springs out and placing them under the electrical penetration wings, these mass terms for node 18 must be modified. The purpose of this modification is to ensure that the model still behaves the same as when all springs and masses were located at node 18. We must ensure that we have:

- 1) The same overall global mass and stiffness
- 2) The same center of rotation

Mass is transformed using the parallel axis theorem:



\bar{I} equals inertia about centroidal axis

$$I_{BB} = \bar{I} + AY^2 \quad \text{Inertia about axis BB}$$

∴ For mass located BB and if we desire to have an inertia of \bar{I} at axis AA, Define

$$I' = \bar{I} - AY^2$$

$$\therefore I_{AA} = I' + AY^2 = \bar{I} \quad \text{rotational}$$

∴ Use translation of centroidal inertia minus the translational mass (distance)²

TITLE _____
 BY RHK DATE 2/2/82
 CHKD. BY PSH DATE 3/1/82



STRUCTURAL
 MECHANICS
 ASSOCIATES
 A Calif. Corp.

PAGE 60 OF JOB No.
 COMMENTS Mass Coordinate
Transformations

Lower Bound Mass

Orig. Node 18 Mass

Orig. Coord.

$$X \text{ Mass} = 1039 \frac{\text{K-sec}^2}{\text{ft}}$$

$$X_G = 81.64 \text{ ft}$$

$$Y \text{ Mass} = 1039 \frac{\text{K-sec}^2}{\text{ft}}$$

$$Y_G = -2.31 \text{ ft}$$

$$Z \text{ Mass} = 940 \frac{\text{K-sec}^2}{\text{ft}}$$

$$Z_G = 565.0 \text{ ft}$$

$$\text{Rot } X \text{ Mass} = 0.9884 \cdot 10^7 \text{ K-sec}^2 \text{-ft}$$

$$\text{Rot } Y \text{ Mass} = 0.1131 \cdot 10^8 \text{ K-sec}^2 \text{-ft}$$

$$\text{Rot } Z \text{ Mass} = 0.3885 \cdot 10^7 \text{ K-sec}^2 \text{ft.}$$

New Coord. of Node 18

$$- \text{sec } p. 52E-1, 52E-2 \quad \left\{ \begin{array}{l} X = 71.70 \\ Y = -2.52 \\ Z = 564.25 \end{array} \right.$$

$$X_{M18} = X_{M6} = 1039 \frac{\text{K-sec}^2}{\text{ft}}$$

$$\Delta X = 81.64 - 71.70 = 9.94'$$

$$Y_{M18} = Y_{M6} = 1039 \frac{\text{K-sec}^2}{\text{ft}}$$

$$\Delta Y = -2.31 - 2.52 = 0.21'$$

$$Z_{M18} = Z_{M6} = 940 \frac{\text{K-sec}^2}{\text{ft}}$$

$$\Delta Z = 565 - 564.25 = 0.75'$$

$$M_{\psi_{X6}} = M_{\psi_{X18}} + M_{Z18} \Delta Y^2 + M_{Y18} \Delta X^2$$

$$\therefore M_{\psi_{18}} = M_{\psi_{X6}} - M_{Z18} \Delta Y^2 - M_{Y18} \Delta X^2$$

Similarly for other two directions:

$$M_{\psi_{Y18}} = M_{\psi_{Y6}} - M_{X18} \Delta Z^2 - M_{Z18} \Delta X^2$$

$$M_{\psi_{Z18}} = M_{\psi_{Z6}} - M_{X18} \Delta Y^2 - M_{Y18} \Delta X^2$$

Values for Lower Bound

$$M_{\psi_{X18}} = 0.9884 \cdot 10^7 - (940)(0.21)^2 - 1039(0.75)^2$$

$$M_{\psi_{X18}} = 0.9883 \cdot 10^7 \frac{\text{K-sec}^2}{\text{ft}}$$

$$M_{\psi_{Y18}} = 0.1131 \cdot 10^8 - (1039)(0.75)^2 - 940(9.94)^2$$

$$M_{\psi_{Y18}} = 0.1122 \cdot 10^8 \frac{\text{K-sec}^2}{\text{ft}}$$

$$M_{\psi_{Z18}} = 0.3885 \cdot 10^7 - 1039(0.21)^2 - (1039)(9.94)^2$$

$$M_{\psi_{Z18}} = 0.3782 \cdot 10^7 \frac{\text{K-sec}^2}{\text{ft}}$$

TITLE _____

BY: EHK DATE 2/2/82CHKD. BY: 254 DATE 3/1/82

STRUCTURAL
MECHANICS
ASSOCIATES
A CALIF. CORP.

PAGE 61 OF _____ Job No. _____COMMENTS MassTransitionUpper Round Mass

New node 18 locations see p. 55

$$X = 42.96$$

$$Y = -3.19$$

$$Z = 562.09$$

Using the previous page $\Delta X = 38.68'$

$$\Delta Y = 0.88'$$

$$\Delta Z = 2.91'$$

For Upper Round Case:

$$M_{\psi_{x,18}} = 0.9884 \cdot 10^7 - 940(0.88)^2 - 1039(2.91)^2$$

$$M_{\psi_{x,18}} = 0.9874 \cdot 10^7 \text{ K-sec}^2/\text{ft.} \quad \checkmark$$

$$M_{\psi_{y,18}} = 0.1131 \cdot 10^8 - 1039(2.91)^2 - 940(38.68)^2$$

$$M_{\psi_{y,18}} = 0.9895 \cdot 10^7 \text{ K-sec}^2/\text{ft.} \quad \checkmark$$

$$M_{\psi_{z,18}} = 0.2285 \cdot 10^7 - 1039(0.88)^2 - 1039(38.68)^2$$

$$M_{\psi_{z,18}} = 0.2330 \cdot 10^7 \text{ K-sec}^2/\text{ft.} \quad \checkmark$$

Use same translational mass as given on previous page